Fall 11-15-2016

Optimized sizing and placing of Distributed Energy Resources (DERs) in an island microgrid using DER-CAM

Bhuwan B. Bastola

Bhuwan Babu Bastola

Candidate

Electrical and Computer Engineering

Department

This thesis is approved, and it is acceptable in quality and form for publication:

Approved by the Thesis Committee:

Andrea Alberto Mammoli, Chair

Jane Lehr, Co-Chair

Olga Lavrova, Member

Optimized sizing and placing of Distributed Energy Resources (DERs) in an island microgrid using DER-CAM

by

Bhuwan Babu Bastola

Bachelors in Electrical Engineering, Tribhuvan University, 2014

THESIS

Submitted in Partial Fulfillment of the
Requirements for the Degree of

Master of Science
Electrical Engineering

The University of New Mexico

Albuquerque, New Mexico

December, 2016

Dedication

To my parents, Laxman Bastola and Sita Devi Bastola, for their love, support, and encouragement.

Acknowledgments

I would like to thank my research supervisor, Professor Andrea Alberto Mammoli, for the wonderful opportunity to work on the project along with his relentless supervision and support throughout the time. I could not have imagined any better supervisor to work with. And without his supportive, inspiring and patient tutorship the thesis would never have been.

I would also like to thank my academic advisor and committee member, Professor Jane Lehr for her time to serve as a committee member. I feel very fortunate to have a such an advisor/mentor thanks to her wonderful support, advices and counseling during my grad school.

Professor Olga Lavrova was such an influential and inspiring to continue my eduction and fuel interests on the area of energy and power systems. I express my warm thankfulness for her support and time serving as a committee member even at her hardship.

My thankfulness and appreciation also goes to Steve Willard, from Electric Power Research Institute (EPRI), for his inspiring supervision this project.

Optimized sizing and placing of Distributed Energy Resources (DERs) in an island microgrid using DER-CAM

by

Bhuwan Babu Bastola

Bachelors in Electrical Engineering, Tribhuvan University, 2014

M.S., Electrical Engineering, University of New Mexico, 2016

Abstract

The electric grid at La Gomera, an island in the Canary archipelago, has been the subject of interest in optimized integration of Distributed Energy Resources (DERs) primarily because of high distribution losses and concerns about complying with emission regulations. Consequently, the utility that operates the island power system wishes to mitigate the problem with installation of renewable and distributed energy sources like PV and battery, which is the focus of this research.

Specifically, the focus of this thesis is to use Distributed Energy Resource - Customer Adoption Model (DER-CAM) to optimize the installation of PV and battery in terms of their sizing and placing. The dynamic electric system at the island is modeled with the information available from different sources and run in DER-CAM. The power flow results from DER-CAM are benchmarked with those provided from Electric Power Research Institute (EPRI) to ensure the modeling of system and running the power flow are reasonable, and then different cases of optimized placing and sizing of PV and battery installation are run. The results are studied on how the

installations enhance performance of the microgrid in terms of costs and emissions and then presented to the utility company for the deployment of DERs.

Contents

List of Figures

List of Tables

Glossary

EPRI	Electric Power Research Institute
DER	Distributed Energy Resource
DER-CAM	Distributed Energy Resource- Customer Adoption Model
PSSE	Power Transmission System Planning Software
DG	Distributed Generation
PV	Photovoltaics
ES	Electric Storage
PCC	Point of Common Coupling
S_{base}	Base power in per unit system
V_{base}	Base voltage in per unit system
pu	Per unit
TMY	Typical Meteorological Year

Chapter 1

Introduction

1.1 Microgrid and Distributed Energy Resources (DERs)

The term "Microgrid" refers to a relatively small sized grid which has a group of interconnected loads and energy resources of its own and can even operate independent of a bigger grid. That said however, it has came out to be a vague term and is often tried to define what it is and what not by many sources. Microgrid, as per DNV KEMA Energy and Sustainability and Peregrine Energy Group [19], is defined as a power distribution network comprising multiple electric loads and distributed energy resources, characterized by all of the following:

- The ability to operate independently or in conjunction with a macrogrid;
- One or more points of common coupling (PCC's) to the macrogrid;
- The ability to operate all distributed energy resources (DER), including load and energy storage components, in a controlled and coordinated fashion, either while connected to the macrogrid or operating independently.

- The ability to interact with the macrogrid in real time, and thereby optimize system performance and operational savings [19].

A purpose of microgrid is well explained as to economically provide electricity to critical loads within the microgrid, and to improve power quality, flexibility, and reliability by integrating and optimizing various sources of energy.

Distributed generation is a feature of microgrid which means the generation is scattered over the electric network system. Distributed Energy Resources (DERs) are smaller sources of energy that in aggregate can supply the load demand. In contrast to the conventional energy generation plants such as coal-fired, natural gas and nuclear power plants, hydropowers, large-scale PV and wind farms which are centralized and have to transmit bulk power from the generating location of the load, DERs are more decentralized or distributed and hence are more flexible and efficient. DERs are also refereed as Distributed Generations (DGs), Discrete Generation or On-site Generation and include following [12]:

- Combined heat power (CHP)
- Fuel Cells
- Hybrid power systems (solar hybrid and wind hybrid systems)
- micro combined heat and power
- Microturbines
- Photovoltaic systems (PVs)
- Small wind power systems
- or any combination of above

Due to the distribution of energy sources across the grid network, a microgrid with DERs has an advantage of smaller distribution losses and greater efficiency in comparison with the conventional centralized grids. Since these energy sources are

mostly clean, renewable and do not emit green house gases like CO_2, their popularity has been soaring these days because of environmental and sustainability issues. In other words, DERs serve to encourage the use of clean and renewable energies. Figure 1.1 shows a simple diagram of operation of microgrid.

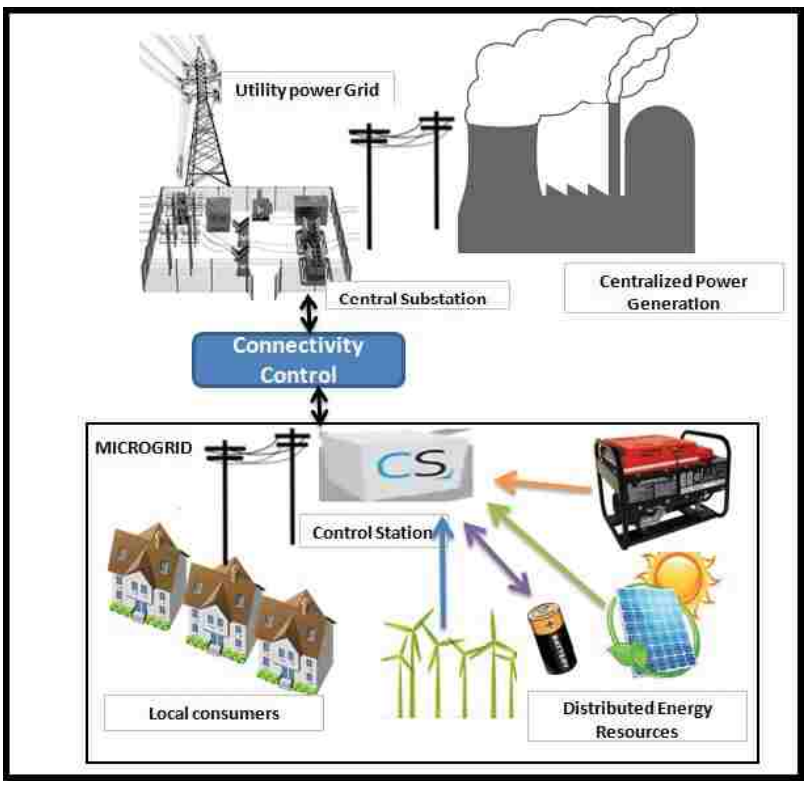

Figure 1.1: Microgrid

Even though the DERs can be simply plugged in into the microgrid, wide ranges of benefits and advantages can be harnessed with a planned and optimized installation and operation of them [19]. The benefits includes improvement of bus voltages along with line loss reduction, reliability enhancement, ancillary services (generation adequacy), emission reduction and fuel cost minimization. In order to maximize the benefits of DERs as described above however, optimal identification of the best DERs along with its size location, manner of interconnection to the system and schedule of deployment has to be done [6]. One of a major question for their integration is

to find the optimized solution for their sizing and placing. The Distributed Energy Resource Customer Adoption Model (DER-CAM) is an example of a tool which can be used to find a practical solution to the problem. The primary focus of this thesis is to find optimized sizing and placing of PV and electric storage in an island microgrid using DER-CAM.

DER-CAM is an optimization tool which has been in development at Lawrence Berkeley National Laboratories (LBNL) since 2000. It takes input information in the form of data for building energy service, electricity and gas tariff data, DER technology data and site weather and minimizes total costs to determine optimal equipment combination and operation. Specifically, DER-CAM sets up an optimization problem which is the total costs of energy, and this is formulated with various costs in microgrid. It solves the optimization problem to determine optimal solution in terms of total costs of energy and/or emissions and that includes the optimized sizing and placing of integrating DERs.

This work is a collaborative project between University of New Mexico (UNM) and Electric Power Research Institute (EPRI) to optimize integration of PV and batteries in an island microgrid using DER-CAM. Necessary information was provided by EPRI and the utility company operating at the island to model the microgrid in DER-CAM and the network is run to study the power flow results and optimizations. The focus of this thesis is to optimize the sizing and placing of PV and batteries after verify the modeling of microgrid in DER-CAM with results from other simulation tools (PSSE in our case).

1.2 Background on modeling and optimization techniques and tools

A microgrid is an integration of various units such as small generator sets, DG units, energy-storage technologies and conventional load. Because of various technologies that could be used, microgrid modeling can vary from one configuration to other depending on the components used [18]. DERs have economic, power quality, flexibility and reliability edge over the conventional generation technologies. However, a planning for the installation and operation of those generation technologies in an effective and optimized way requires tools/techniques that allow complex modeling and optimization for their integration into the grid network.

In conventional way to model the dynamics of an autonomous microgrid system, the dynamics of all DG units were approximated by a first order linear model with time constant and a gain factor. Time domain analysis is carried out after developing transfer functions of various components of microgrid [18].

Microgrid Design Toolkit (MDT) is a design tool that helps to model and optimize the decisions for upgrading microgrid at the beginning level in terms of the user-defined objectives and constraints such as cost, performance and reliability. It can search through large design specifications effectively for alternative energy schemes that would be efficient. It can also facilitate the investigation of simultaneous impacts of several design decisions and derive defensible and quantitative evidence for decisions [1].

Microgrid/Grid Layout Optimizer is another tool that can be used in the optimization of a microgrid. It intends to develop the optimally efficient topologies that can be installed on a microgrid satisfying the targeted static reliability criterion. The primary purpose of this tool is to design the preliminary layout of a microgrid that

can in turn be refined by more sophisticated tools such as Microgrid Design Toolkit [1].

HOMER Energy (Hybrid Optimization of Multiple Energy Resources) is one of a global standard microgrid tool that excels in all simulation, optimization and sensitivity analysis. Microgrids that can include renewable power sources, storage and fossil fuel based generations can be modeled effectively, optimized and carried out various analysis of the economical, financial and power quality analysis. It was originally designed at National Energy Laboratory for the village power program [2].

DER-CAM (Distributed Energy Resources Customer Adoption Model) is a decision support tool for investment and planning of Distributed Energies on microgrids and buildings. The problems addressed by it falls in the Mixed Integer Linear Programming (MILP) and finds the optimal solution in terms of investments and planning while minimizing the total energy costs, carbon dioxide minimizations or an objective that considers both [20]. The overview of DER-CAM operation is shown in Figure 1.2.

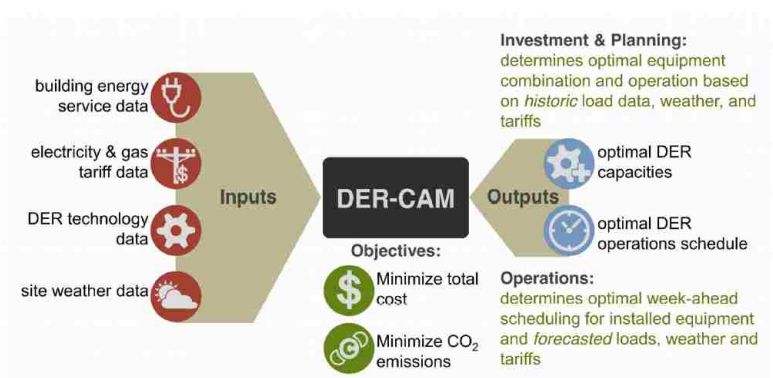

Figure 1.2: Overview of DER-CAM

This thesis uses DER-CAM to optimize the integration of DERs into microgrid. The variables used to model and optimize the microgrid could be both continuous

like a size of PV installations or integer like a number of specified generation set. DER-CAM uses General Algebraic Modeling System (GAMS)-high-level modeling system for mathematical programming and optimization- to run the optimization problem and find solutions [10]. There were two modes of operation of DER-CAM:

- Investment and Planning DER-CAM
- Operations DER-CAM

DER-CAM is run in Investment and Planning mode in this thesis to find optimal investment decisions for a representative year. DER-CAM considers the following inputs [5]:

- Network data: Lengths of cable sections, impedance and admittance matrices and branch capacities.
- The end-use hourly load profiles: electricity-only load defined over three data types: week days, weekend days and peak days.
- Electricity tariff, fuel prices and other relevant financial data.
- Generation rating, capital cost, operation and maintenance costs, minimum loading, efficiency and other necessary information about the generation technologies as well as similar information about the DGs that were considered be picked up during optimization.

The basic outputs that were determined by the DER-CAM:

- Optimal capacity of DERs at a given site.
- Energy Dispatch of all the generation technologies.
- Detailed economic results like the cost of energy in each locations and fuel costs.

In general, an alternating current power flow model is used to carry out the power flow studies in these tools. It is a non-linear system which describes the power flow into the buses as a function of square of applied voltages. Because of it, the power flow were calculated through iterations using numerical analysis up to desired accuracy. The goal of power flow study is to calculate the real and reactive power flow into each buses and their voltage magnitude and angle.

The process to solve the power-flow begins with identifying the known and unknown variables of the system out of the real power (P), reactive power (Q), voltage magnitude (V) and voltage angle (θ). These information depends upon the type of bus and are initial assumptions in power flow iterations. A load bus (where no any generators were connected) would have the P and Q given while V and θ were missing. Similarly, a generator bus (where at least one generator is connected and is not slack bus) will have the information of P and V and Q and θ were to be calculated. A slack bus is arbitrarily selected generator bus [17] and is the only bus for which the system reference phase angle is defined.

Nodal Admittance Matrix (Ybus or Ymatrix) is a matrix which enlists the network information(admittances of transmission cables) and is one of the basic data requirements for the power flow calculation in power system.

$$\text{Ybus} = \begin{pmatrix} Y_{11} & Y_{12} & Y_{13} & ... & Y_{1N} \\ Y_{21} & Y_{22} & Y_{23} & ... & Y_{2N} \\ Y_{31} & Y_{32} & Y_{33} & ... & Y_{3N} \\ ... & ... & ... & ... & ... \\ Y_{N1} & Y_{N2} & Y_{N3} & ... & Y_{NN} \end{pmatrix}$$

The order of admittance matrix is $N \times N$ for a power system with 'N' number of buses. Each bus in the network is connected through transmission line or lines. The equations used to construct Ybus come from the application of Kirchhoff's current

law and Kirchhoff's voltage law. Impedance matrix (Zbus) is usually formed by inverting the Ybus. The steps to calculate Ybus can be summarized as follows:

- First, the single line diagram is converted to an impedance diagram.
- Next, all the voltage sources were converted to their equivalent current source representations.
- Finally, the Y matrix is formulated using the following basic equations:

  1. Diagonal elements:

  Y_{11}= y_1 + y_{12} + y_{13} + y_{14} + ... y_{15}

  Y_{22}= y_2 + y_{21} + y_{23} + y_{24} + ... y_{2n}

  Y_{nn}= y_n + y_{n1} + y_{n2} + y_{n3} + ... y_{nn-1}

  2. Non-Diagonal elements:

  Y_{12}= -y_{12}

  Y_{23}= -y_{23}

  where

  y_{ij} refers to the branch admittance between bus i and bus j.

Real and Reactive power balance equations are used to iterate the known and unknown variables with the latest values of unknown variables to get more closer results for them. Consecutively, they were as follows [17]:

$$P_k = \sum_{j=1}^{N}(|V_k||V_j|G_{kj}Cos(\theta_k - \theta_j) + B_{kj}Sin(\theta_k - \theta_j))$$

$$Q_k = \sum_{j=1}^{N}(|V_k||V_j|G_{kj}Sin(\theta_k - \theta_j) - B_{kj}Cos(\theta_k - \theta_j))$$

where,

P_k = real power injected at k^{th} bus.

Q_k = reactive power injected at k^{th} bus.

V_k = voltage magnitude at k^{th} bus.

The above equations are non-linear and require sophisticated numerical methods to solve them, and hence makes it more complex to integrate with optimization. Due to the complexity because of nonlinear power equations, several efforts has been devoted to design of numerical methods to solve power flow equations [13].

A similar approach is taken into account to linearly approximate the power flow results in DER-CAM. It derives an explicit approximate solution to a non-linear power flow model of a balanced distribution system by linearizing active and reactive power demands of the PQ buses [7]. Accordingly, the power flow equations were linearized to the following equations.

Voltage Equations:

$$Vr_m(t) = V_o + 1/V_o \sum_{n \neq slack} (Zr_{m,n}(Pg_n(t) - Pl_n(t)) + Zi_{m,n}(Qg_n(t) - Ql_n(t)))$$

$$Vi_m(t) = 1/V_o \sum_{n \neq slack} (Zi_{m,n}(Pg_n(t) - Pl_n(t)) - Zr_{m,n}(Qg_n(t) - Ql_n(t)))$$

where

V_o = slack bus voltage.

Vr_m = real voltage at m^{th} node.

$Zr_{m,n}$ = real impdedance between m^{th} and n^{th} node.

$Zi_{m,n}$ = imaginary impdedance between m^{th} and n^{th} node.

$Pg_n(t)$ = Active power generated at n^{th} node.

$Qg_n(t)$ = Reactive power generated at n^{th} node.

Current Equations:

$$Ir_{m,n}(t) = Yr_{m,n}(Vr_n(t) - Vr_m(t)) - Yi_{m,n}(Vi_n(t) - Vi_m(t))$$

$$Ii_{m,n}(t) = Yi_{m,n}(Vr_n(t) - Vr_m(t)) + Yr_{m,n}(Vi_n(t) - Vi_m(t))$$

where

$Ir_{m,n}$ = real current flowing between m^{th} and n^{th} node.

$Ir_{m,n}$ = imaginary current flowing between m^{th} and n^{th} node.

$Yr_{m,n}$ = real admittance between m^{th} and n^{th} node.

$Yi_{m,n}$ = imaginary impdedance between m^{th} and n^{th} node.

Power Equation:

$$\sum_{m} Pg_m(t) = \sum_{m} Pl_m(t) + \sum_{m}\sum_{n} Zr_{m,n} {I_{m,n}}^{sq}(t)$$

where

$$\sum_{m}\sum_{n} Zr_{m,n} XI_{m,n}{}^{sq}(t) = Loss$$

.

Since the loss equation is non-linear (as loss depends on square of the current), the square of current is approximated using the following equations [15] as shown in the Figure 1.3 :

$${Ir_{m,n}}^2(t) = \sum_{k}(2k-1)(Ir_{m,n})/k Ir_{m,n,k}(t)$$

$${Ii_{m,n}}^2(t) = \sum_{k}(2k-1)(Ii_{m,n})/k Ii_{m,n,k}(t)$$

where

k is the number of current segments during linearizion.

The linearized voltage equation suggests that approximating voltage of a node does not require any information about its connection to slack bus in impedance matrix. This is expected to serve as an advantage in order to calculate Zbus from Ybus. Since Ybus is not readily invertible, it can be truncated by removing the row

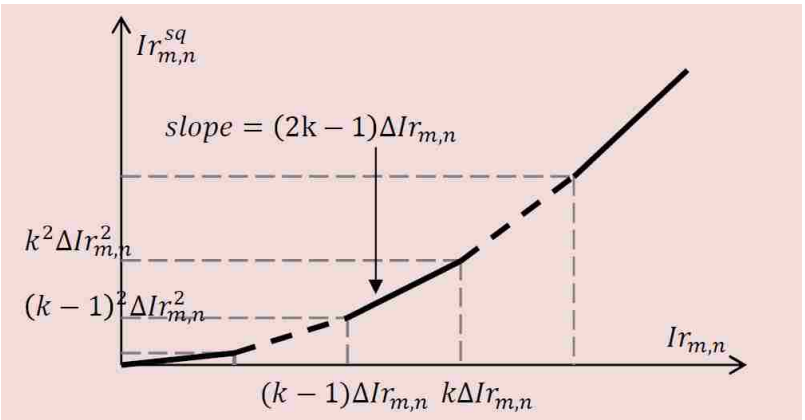

Figure 1.3: Linearizion of square of current for loss approximation

and column corresponding to slack bus, and then inverted. The resulting matrix can be added with a row and column consisting zeros to form a Zbus. It actually misses the admittance information about the connections to slack bus but since the equations do not use it anyway, the Zbus constructed that way works in DER-CAM.

1.3 Challenges in modeling microgrid and optimization

The first challenge in modeling the microgrid is to gather necessary data for it. Data and information has to be enough to model in DER-CAM otherwise the optimization results will be based on assumptions that will decrease the credibility of solutions.

For example, information like the loads in kW provided only on the feeder locations has to be allocated at different points on the network associated with towns according as the population distribution on the island. This way the network and load distributions can be made more diverse.

Because of the complexity of modeling, there were many inputs to be given to

DER-CAM in order to model the entire microgrid and all necessary information might not acknowledged right at the start. Such data will have to be asked after realizing their need, and they might not be guaranteed to be provided right away. In such times, the estimations and assumptions are made by discussions with EPRI.

DER-CAM has to be accessed using remote logging. As the result, the work is highly dependent on Internet which poses risks of setbacks. Interruptions in the server computer can also hinder the work.

1.4 The structure of this thesis

In Chapter 2, a detailed description of La Gomera island and its microgrid was presented. The island microgrid that was required to be optimized in terms of DERs installations is self operating with its own diesel generators and is targeted to be replaced by clean and renewable energy resources in future.

In Chapter 3, all the necessary information and data required to model the electrical network, run the power flow and optimize the integration of DERs were presented. They came from different sources like EPRI, companies overseeing generations and distributions at the microgrid and online resources. The information was then processed to characterize and model microgrid in Chapter 4. At the end of this chapter, input data to the DER-CAM characterizing the microgrid were prepared.

In Chapter 5, the system that was run in PSSE- a power flow simulation tool- by EPRI was run in DER-CAM. Different settings such as parameters, simulation and other DER-CAM settings were discussed. The power flow results were then compared and studied against those from PSSE to make sure that the results from DER-CAM were reasonable. After deciding the two models were in reasonable agreement, the model was then reconfigured in Chapter 6 to a closer model of existing network in La Gomera. Base Case run was also carried out which refers to the case of running the system with currently existing technologies.

In Chapter 7, the system was subjected to optimization with different cases of installation of PV and battery. These cases include different combinations of PV and electric storages installation in different specified locations to look for optimized results of them. The results were then studied and analyzed in terms of several aspects such as total costs of energy, emissions of C02.

Finally in Chapter 8, conclusions and suggestions were presented.

Chapter 2

Background

2.1 La Gomera

2.1.1 General

La Gomera, as shown in Figure 2.1, is one of the seven main islands of Canaries, Spain located in Atlantic ocean on the west of north Africa. It has a roughly circular area with a diameter of around 22 kilometers. It belongs to the province Santa Cruz de Tenerife of Kingdom of Spain with the capital San Sebastian de La Gomera.

Figure 2.1: Map of La Gomera

The tourism based island had a population of reportedly around 21950 in 2009 residing over the 370 km^2 area of the whole island. Even though the population is scattered over the island, the major towns were San Sebastian, El Molinito, Vallehermoso and Valle Gran Rey [16].

Politically, it is divided into six municipalities as follows:

- Agulo
- Tecina
- San Sebastian de la Gomera
- Valle Gran Rey
- Vallehermoso

2.1.2 Energy Scenario of La Gomera

La Gomera is almost 100 percent dependent on petroleum for its energy demands with almost no energy diversification. The primary sources of energy were fossil fuel and small amount of renewable energy in the form of wind and solar. Fossil fuel is the major source of energy for almost every ways on the island. Diesel and gasoline were used in transportation sector whereas LPG (Liquefied Petroleum Gas) is used in the residential sectors. Diesel is the fundamental and most used fuel in the whole island, and is used heavily for the generation of electricity.

The rules, regulations and other issues concerned with energy and power at La Gomera are overseen and monitored through various institutions at different levels.

The **Ministry of Industry, Energy and Tourism**, a government body of Spain, is the responsible for proposing, administrating and regulating plan, policies and laws governing the energy, industry and tourism in Spain, and La Gomera [4].

Institute of Energy Diversification and Energy Savings (IDAE) is a public company under the aforementioned ministry which looks after the close monitoring of energy sector as well as promoting energy efficiency, how were they complying with national and European standards [4].

National Energy Commission of Spain is another national level of the country which works to make sure the transpwerency of things related to electricity for the sake of advantages to other parties trying to operate over there and free competition on energy for its healthy promotion [4].

Endesa, currently a subsidiary of Italian energy giant **ENEL**, is a company in Spain that is operating electricity industries. Endesa owns the thermal plant located in the largest settlement of La Gomera, San Sebastian de la Gomera. It consists of altogether ten- eight fixed and two movable- generator sets operating with diesel [8].

DIRECTIVE 2009/28/EC of the European Parliament and of the council of 23 April 2009 lays a legal framework on Europe including La Gomera for the increased use of energy from renewable resources, decreased emission of greenhouse gases, decentralization of energy sources especially renewable ones and check the energy dependence of communities with others. It states, "The control of European energy consumption and the increased use of energy from renewable sources, together with energy savings and increased energy efficiency, constitute important parts of the package of measures needed to reduce greenhouse gas emissions and comply with the Kyoto Protocol to the United Nations Framework Convention on Climate Change, and with further Community and international greenhouse gas emission reduction commitments beyond 2012. Those factors also have an important part to play in promoting the security of energy supply, promoting technological development and innovation and providing opportunities for employment and regional development, especially in rural and isolated areas." [11]

The European Union also has an ambitious plans on increasing the proportion of renewable and clean energies, decreasing the emissions of green house gases like CO_2 and enhancing the efficiency. It can be summarized by the 20-20-20 objective adopted by it that were based on the three pillars leading European energy policy: Security of supply, competitive markets and sustainability. The 2020 energy goals were to have a 20% (or even 30%) reduction in CO_2 emissions compared to 1990 levels, 20% of the energy, on the basis of consumption, coming from renewable energy sources and a 20% increase in energy efficiency [14].

2.1.3 Electrical Microgrid

The electrical network across the La Gomera island is comprised of a single microgrid. Electricity is generated centrally at a place at Bus 1 which is near the capital San Sebastian on east side of island and is distributed to the scattered loads across the

island through five distribution feeders: Feeder 1, Feeder 2, Feeder 3, Feeder 4 and Feeder 5.

Generation

The electricity generation at La Gomera is centralized and is done at Central térmica El Palmar (English translation: Thermal Plant El Palmar) [8]. The thermal power plant at the place is located at the biggest city of La Gomera: San Sebastian de La Gomera as shown in Figure 2.2. Its consist of 8 fixed thermal plants and 2 mobile diesel generators and is modeled as Generator Bus throughout this thesis.

Figure 2.2: Central térmica Bus 1 (Thermal Central Bus 1)

The generation units has the following specifications:

- Unit 12 is a thermal plant and has the rated capacity of 1.4 MW,6.6 kV and internal machine reactance of 0.237 at the machine power base.
- Unit 13 is also a thermal plant has the rated capacity of 1.4 MW, 6.6 kV but the internal machine reactance is 0.25 pu at the machine power base.
- Unit 14 and Unit 15 were two thermal plants with the capacity of 1.84 MW at 6.6 kV and internal reactance of 0.21 pu at the machine base power.
- Unit 16 and 17 were also thermal plants with the rated capacity of of 2.51 MW at 6.6 kV and internal reactance of 0.223pu at the machine base power.
- Unit 18 and 19 were also thermal plants with the capacity of 3.1 MW, 6.6 kV and internal reactance of 0.2 pu at the machine base power.

All of these generators are connected to the Bus 1 that is operating at voltage level of 20 kV through step up transformers. Currently a very small proportion of the total energy generated- about 1.15%- has been contributed by renewable energy, consisting primarily wind which has been neglected on this work.

The electricity generated by the generators is transmitted through distribution lines operating the the voltage level of 20 kV. Figure 2.3 as below shows the electrical grid map of the distribution lines.

Most of the loads at La Gomera are household appliances because La Gomera's biggest industry is tourism. Together with inconvenience in DER-CAM to work on reactive power, this made us easy to assume the power factor of the load 1 and hence neglect the reactive power demand at load side. The peak load at the island was approximately 12 MW in 2014, and the total energy produced on the same year 66.674 GWh of electricity.

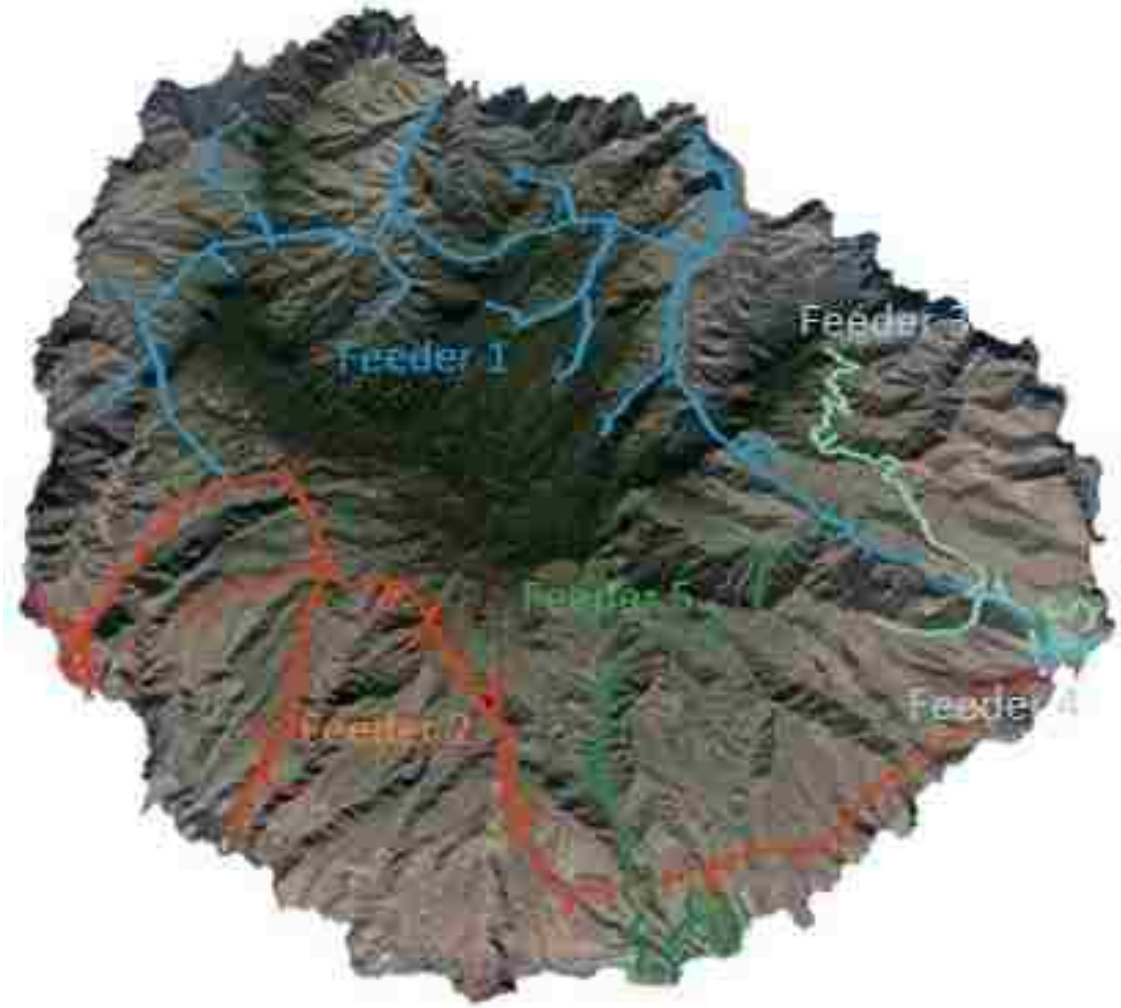

Figure 2.3: Electrical Microgrid network at La Gomera

2.2 Purpose of Study

The measured distribution losses in the electrical system of La Gomera is substantially high- about 8.7% of the power produced by the generators is dissipated as loss. Electricity generation at a single point with transmission lines of several kilometers at the voltage level of 20 kV serving scattered load at different parts of the island makes the system lossy. The island has also embraced increasing restrictions over

the emission of green house gases and need to increase the proportion of renewable energy as regulated both by Spain and European Union. Most of those regulations can be summarized by the '20-20-20' objective. It states that the year 2020 energy goals were to have a 20% reduction in CO_2 emissions compared to 1990 levels, 20% of the energy, on the basis of consumption, coming from renewable and a 20% increase in energy efficiency. Currently, the island has bwerely 1.15% of total energy consumed coming up from renewable [14]..Because of this, utility company operating at La Gomera wishes to install PV and batter system

Deployment of renewable energy sources like PV and/or electric storage on the island would help the utility confront both the above challenges. However, places and sizes of them are difficult things to figure out in terms of cost and performance optimization. Finding their optimized size and place to install is the primary objective of this thesis. However, in order to characterize and model the whole electric system of the island, from generators to transformers, transmission lines, distribution feeders and loads along with the environmental factors such as temperature, solar insolation and wind speed, it cannot be expected to go easy with traditional approaches- without the assistance of computer tools.

This study, thereby, deploys DER-CAM in order to research over the selection of size and the location of PV and if possible battery installation, so as to see how the new system would put up financially and in terms of CO_2 emissions against than the current lossy system.

Chapter 3

Information and Data

System characterization of the microgrid and modeling it were the fist steps on the project and thesis. First the data and information such as generation specifications, cable lines, line lengths and parameters, transformer data and loads were collected from EPRI and the utility companies.

EPRI had modeled the microgrid and ran the power flow in PSSE (Power Transmission System Planning Softwwere). PSSE is an integrated, interactive tool developed by Siemens for simulating, analyzing, and optimizing power system performance. The information they used to ran the power flow in it was also provided to us.

The 14-node configuration had three types of buses: slack bus, PQ bus (or load bus) and PV bus. As seen from the table below, the bus no. 1 was set as a slack bus whereas the rest of buses were assigned as load bus, with the non-load nodes set as zero load.

3.1 Nodal Information

Table 3.1 shows the data about detailed information of node with 13 buses, together with those where generators were connected to. It consists of the information such as the type of bus (slack, load or generator), the voltage rating in kV and the voltage magnitude and angle during the power flow simulation in PSSE. It also shows the number of generators that were set ON/OFF during the simulation, and those kept off-line were neglected in our project.

Also, one line diagram that was used to model the microgrid for its simulation in PSSE was received from EPRI which mapped the locations used by them according as the buses as listed in above Table 3.1. It is shown as in Figure 3.1

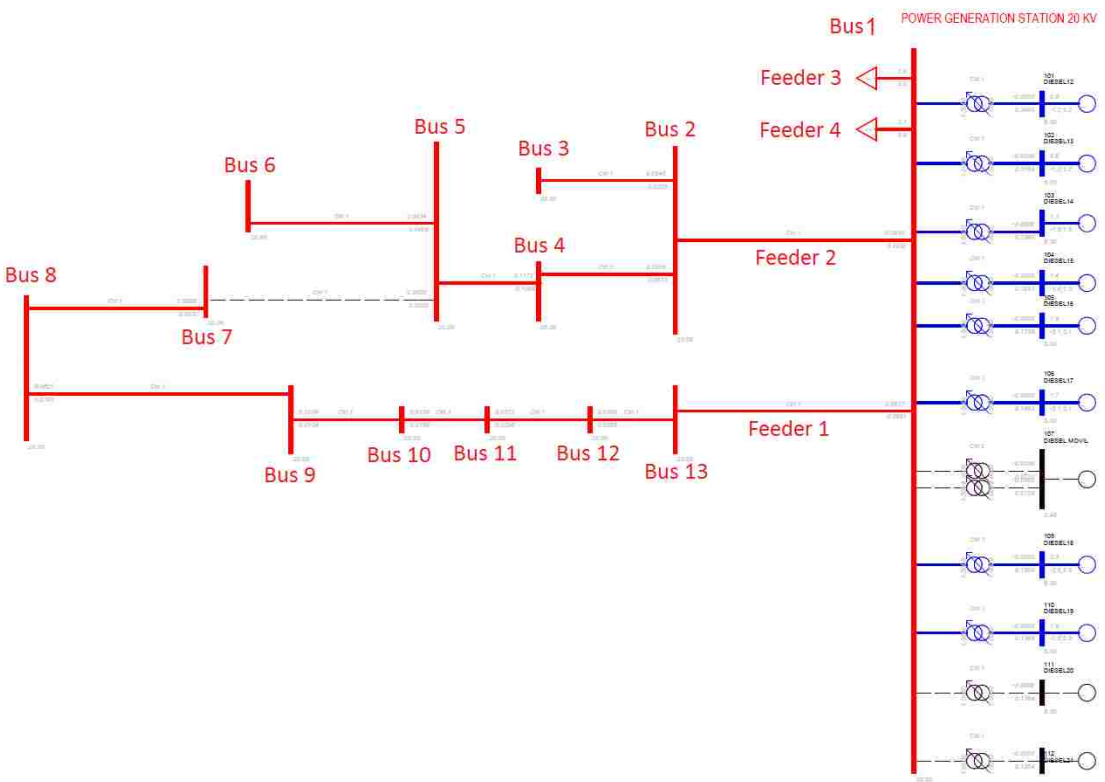

Figure 3.1: One Line Diagram received from EPRI

Table 3.1: Node data from EPRI

Bus Number	Base kV	Code	Voltage (pu)	Angle (deg)
1	20	3	1.0471	-0.93
2	20	1	1.0238	-1.89
3	20	1	1.0207	-1.9
4	20	1	1.0096	-2.24
5	20	1	0.9794	-3.03
6	20	1	0.969	-3.31
7	20	1	0.9794	-3.03
8	20	1	1.0245	-1.39
9	20	1	1.0282	-1.3
10	20	1	1.0297	-1.28
11	20	1	1.0315	-1.23
12	20	1	1.0352	-1.15
13	20	1	1.0389	-1.09
101	6.3	4	1	0
102	6.3	4	1	0
103	6.3	4	1	0
104	6.3	2	1.055	0.15
105	6.3	2	1.055	0.59
106	6.3	2	1.055	0.36
107	0.4	4	1	0
109	6.3	3	1.055	0
110	6.3	4	0.99	-0.03
111	6.3	4	1	0
112	6.3	4	1	0
113	12	4	1	0

Legend

1	Load (PQ) bus
2	PV Bus
3	Slack/Swing
4	Disconnected

3.2 Generation

Buses 101 to 113 in Table 3.1 were the buses where different generators were connected. All of them were operating at the voltage level of 6.3 kV except those

connected to Bus Number 107 and 113. The further information regarding each generator's unit rated power and their numbers as deployed are shown in the Table 3.2.

Table 3.2: Generator Specifications from EPRI

Diesel Genset	no of units	Unit power kW	Total power kW
12 & 13	2	1400	2800
14 & 15	2	1840	3680
16 & 17	2	2510	5020
18 & 19	2	3100	6200
Mobile 2	1	1060	1060
Mobile 3	1	970	970

All the generators were diesel-based and the fuel price for them were set at €689.83/ton for January to June and €616.44/ton for rest of the months.

All these generators were connected to the Bus 1 through step-up transformers. The detailed information about transformer reactances and resistances were provided in Figure 3.2. The base power values for each transformers were also provided in the 'Rate' column of the figure. The information was used to incorporate electrical properties of transformers in while modeling of the microgrid.

3.3 Distribution

Information like length of cables, their resistances and reactances, branch capacities and others were required to model and simulate the microgrid. Table 3.3 summarizes the information provided by EPRI regarding the length of each transmission sections between the given nodes in meters. It also gives the information about line parameters (resistances and reactances) in per unit with the power base of 10 MVA and voltage base of their respective rated voltages. These values were directly used by PSSE to formulate the impedance and admittance matrices and subsequently run

From	From Bus	To Bu	To Bus	Specified R	Specified X	Rate
1	ELPALMAR	101	DIESEL12	0.000000	0.346500	2.0
1	ELPALMAR	102	DIESEL13	0.000000	0.278500	2.0
1	ELPALMAR	103	DIESEL14	0.000000	0.236000	2.5
1	ELPALMAR	104	DIESEL15	0.000000	0.193330	3.0
1	ELPALMAR	105	DIESEL16	0.000000	0.173610	3.6
1	ELPALMAR	106	DIESEL17	0.000000	0.149250	4.0
1	ELPALMAR	107	DIESEL MO	0.000000	0.572000	1.0
1	ELPALMAR	107	DIESEL MO	0.000000	0.572000	1.0
1	ELPALMAR	109	DIESEL18	0.000000	0.136360	4.4
1	ELPALMAR	110	DIESEL19	0.000000	0.136360	4.4
1	ELPALMAR	111	DIESEL20	0.000000	0.136360	4.4
1	ELPALMAR	112	DIESEL21	0.000000	0.136360	4.4
8	VHERMOS	113	VHERMOS	50.000000	0.080000	10.0

Figure 3.2: Transformer Information

the power flow.

Table 3.3: Branch Information from EPRI

From Bus	To Bus	R (pu)	X (pu)	Length (m)	Branch Capacity (MVA)
1	2	0.062	0.093	9700	11.6
1	13	0.083	0.0661	6300	7
2	3	0.054	0.022	3200	4.7
2	4	0.055	0.0513	5200	8.7
4	5	0.117	0.1095	11100	8.7
5	6	0.053	0.0499	5100	8.7
5	7	0.002	0.002	200	8.7
7	8	0.1	0.0933	9500	8.7
8	9	0.082	0.0767	7800	8.7
9	10	0.016	0.0104	1000	6.8
10	11	0.017	0.0166	1700	8.7
11	12	0.037	0.0298	2800	7
12	13	0.038	0.0268	2600	6.7

The last column of the table is rated branch capacity of different sections in MVA. Branch capacity refers to the rated capacity at which the cable can transmit the power under normal conditions and were crucial to determine current carrying capacities of the sections. Since loss approximation for a line uses the line current normalized using branch capacity in DER-CAM, these values affects line loss results.

3.4 Load

An hourly data of load profile for all the nodes were provided from EPRI for each feeder lines which is required to model the load in DER-CAM. Different load centers on feeder lines were recognized from Google Earth according to big settlement areas nearby. The load data of feeder lines were then broken down into those load centers proportional to their population sizes. Table 4.6 Load Table I and Table 4.7 Load Table II shows the load data in kilowatt (kW) for different buses in the network. The data is only shown for a single day due to the page-layout constraints. DER-CAM required load data for a whole year which we had. These data were later on processed to be fitted into DER-CAM. Bus no. 15 and 16 refers to those buses on the Feeder 3 and 4 that were taken into account later in 17-Nodes configuration.

Table 3.4: Load Table I (in kW) from EPRI

hour	Bus 3	Bus 4	Bus 5	Bus 7	Bus 9
1	596.00	798.64	149.00	63.90	653.88
2	570.25	764.14	142.56	69.19	708.09
3	538.00	720.92	134.50	65.41	669.39
4	493.00	660.62	123.25	57.97	593.24
5	484.28	648.93	121.07	63.90	653.88
6	484.28	648.93	121.07	56.44	577.57
7	505.69	677.63	126.42	65.41	669.39
8	501.36	671.82	125.34	60.13	615.33
9	493.00	660.62	123.25	46.30	473.84
10	587.64	787.44	146.91	56.44	577.57
11	658.76	882.74	164.69	61.20	626.30
12	667.12	893.94	166.78	58.51	598.72
13	634.81	850.64	158.70	56.44	577.57
14	611.23	819.04	152.81	55.90	572.09
15	622.12	833.64	155.53	60.13	615.33
16	606.89	813.24	151.72	57.97	593.24
17	565.92	758.33	141.48	54.83	561.12
18	557.56	747.13	139.39	51.07	522.57
19	658.76	882.74	164.69	56.99	583.21
20	858.69	1150.64	214.67	84.09	860.56
21	807.13	1081.55	201.78	88.93	910.07
22	759.59	1017.85	189.90	88.93	910.07
23	684.51	917.24	171.13	79.87	817.31
24	606.89	813.24	151.72	66.50	680.52

Table 3.5: Load Table II (in kW) from EPRI

hour	Bus 6	Bus 8	Bus 15	Bus 16
1	1788.00	726.08	1309.96	1082.98
2	1710.75	786.28	1263.25	1178.13
3	1614.01	743.31	1166.02	1190.24
4	1479.01	658.75	1129.69	1095.09
5	1452.83	726.08	1022.08	1082.98
6	1452.83	641.35	973.30	1046.30
7	1517.08	743.31	1022.08	1034.19
8	1504.08	683.28	973.30	1095.09
9	1479.01	526.16	936.97	924.86
10	1762.93	641.35	1141.80	902.37
11	1976.29	695.46	1153.91	985.41
12	2001.35	664.84	1334.18	1058.41
13	1904.42	641.35	1309.96	1129.69
14	1833.68	635.26	1370.85	1117.23
15	1866.36	683.28	1490.57	1251.14
16	1820.68	658.75	1358.74	985.41
17	1697.75	623.08	1141.80	924.86
18	1672.68	580.27	1178.13	924.86
19	1976.29	647.61	1395.07	997.52
20	2576.06	955.58	1575.68	1141.80
21	2421.38	1010.56	1731.73	1251.14
22	2278.77	1010.56	1707.51	1239.03
23	2053.53	907.56	1539.01	1178.13
24	1820.68	755.66	1287.81	1058.41

Chapter 4

System Characterization and Modeling

The microgrid at La Gomera was modeled with the information and data received from EPRI and the utility companies. The raw data provided had to be processed as per the needs in DER-CAM. The characterization and modeling were summarized as follows:

4.1 Node Characterization

The characterization and modeling in DER-CAM was done first by giving location numbers for each nodes in the network. Therefore, the location numbers starting from 1 (that is Loc1, Loc2, etc.) were assigned radially from the point of generation as shown in the following table. That way, Generator Bus became loc1, Bus 1 became loc2 and so on. Loc1 was referred as the slack bus in our modeling in DER-CAM.

EPRI modeled the microgrid with 13 nodes and generator buses in PSSE and had not taken into account Feeders 3,4 and 5. Because the time EPRI modeled and

ran the power flow simulation, it did not have the information about those feeders. Thereby, even though it would be taken into account those feeders in the power flow and optimization later on, first the system on the DER-CAM is modeled with only those 14 nodes for benchmarking with PSSE. The purpose of 14-nodes system characterization and modeling was to approximate the power flow results of the microgrid and compwere them with that of PSSE to make sure that the comparison look reasonable and the power system characterization and modeling in the DER-CAM was done in a right way.

We have 13 generators from Bus no. 101 to Bus no. 113 as shown in Table 4.1, out of which there were 8 fixed generators. Since only fixed generators were usually operating and others were kept offline in PSSE simulation, only those 8 fixed generators were considered in DER-CAM. All these generators were lumped into a single bus called Generator Bus (loc1). The base voltage rating of this bus was set at 6.3 kV.

The new Node table with their location numbers for DER-CAM is summarized in Table 4.1:

4.2 One Line Diagram

In order to characterize and model the microgrid with simplicity, making an one-line diagram of the network is considered as the first step in tackling the problem. Before going for the one line diagram, first the nodes were identified and numbered as of the location numbers for DER-CAM. They were labeled as in the Fig 4.1 and one line diagram is shown in Fig 4.1.

Table 4.1: Location Table for 14-node configuration

Bus Number	Location No.	Base kV	Code
GENERATION BUS	1	6.6	3
1	2	20	1
2	3	20	1
3	4	20	1
4	5	20	1
5	6	20	1
6	7	20	1
7	8	20	1
8	9	20	1
9	10	20	1
10	11	20	1
11	12	20	1
12	13	20	1
13	14	20	1

Code :

1	Load (PQ) Bus
2	Generator (PV) Bus
3	Slack Bus

4.3 Formation of 14-Node Branch Data

In order to create the admittance (Ybus) and impedance Matrix(Zbus), line parameters resistance (R) and reactance (X) were required in per unit system. All the branch parameters that were used in PSSE were provided to us. Since the simulation in PSSE was based on S_{base} of 10 MVA, all those values except that between the Generator Bus (loc1) and Bus 1 (loc2) were in per unit with common base power of 10 MVA and they were ready to be used for the formulation of Y/Z matrices. However, calculation was required to convert all the generator reactances into a single equivalent value of connection between the Generator Bus (loc1) and Bus 1 (loc2) and in the common base power of 10 MVA.

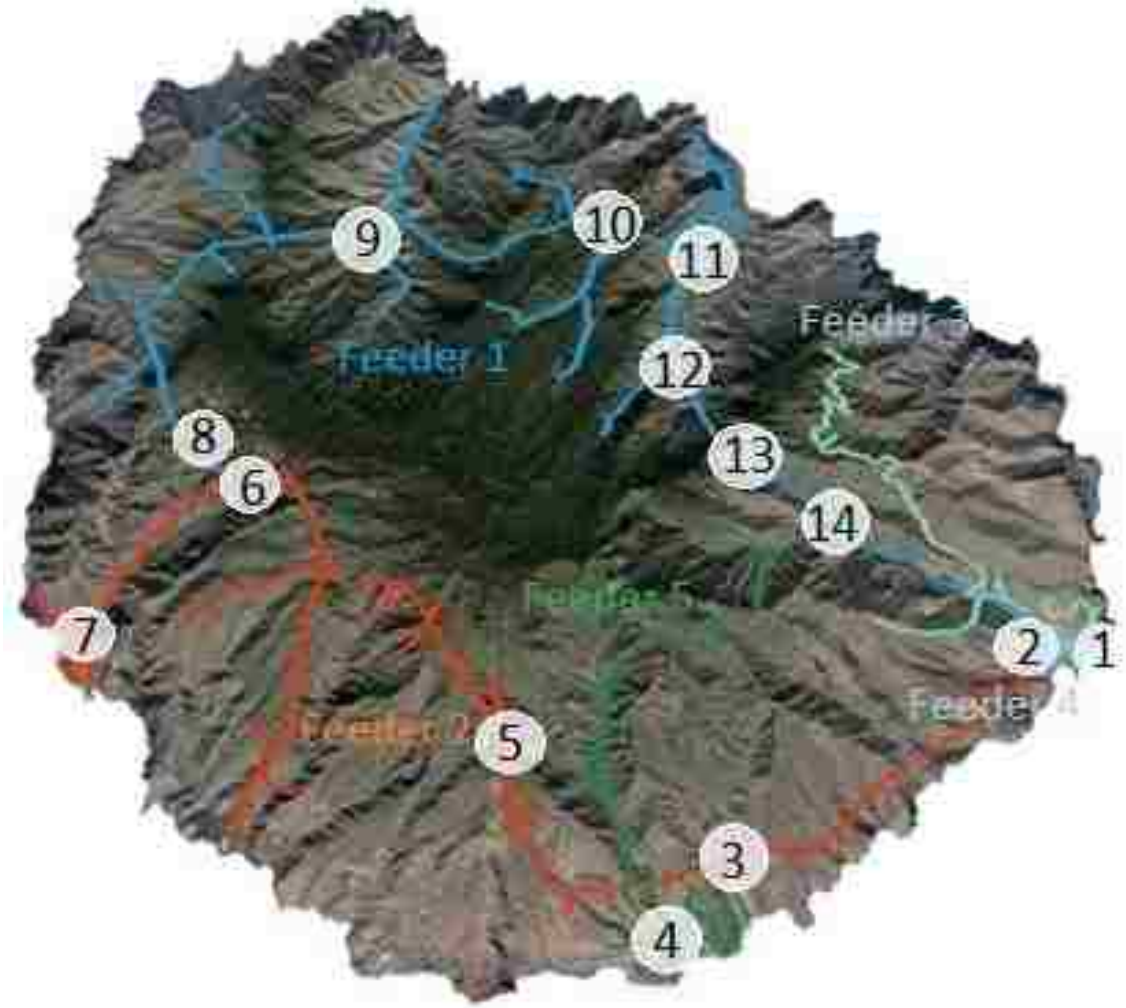

Figure 4.1: 14 Nodes on La Gomera

Reactances of 8 fixed generators- which were kept online in PSSE simulation- and their base values of power were shown in the following table Table 4.2.

Now, using the formula for per unit conversion with new base value of power, Sbase=10 MVA, the new per unit reactances of generators were given by,

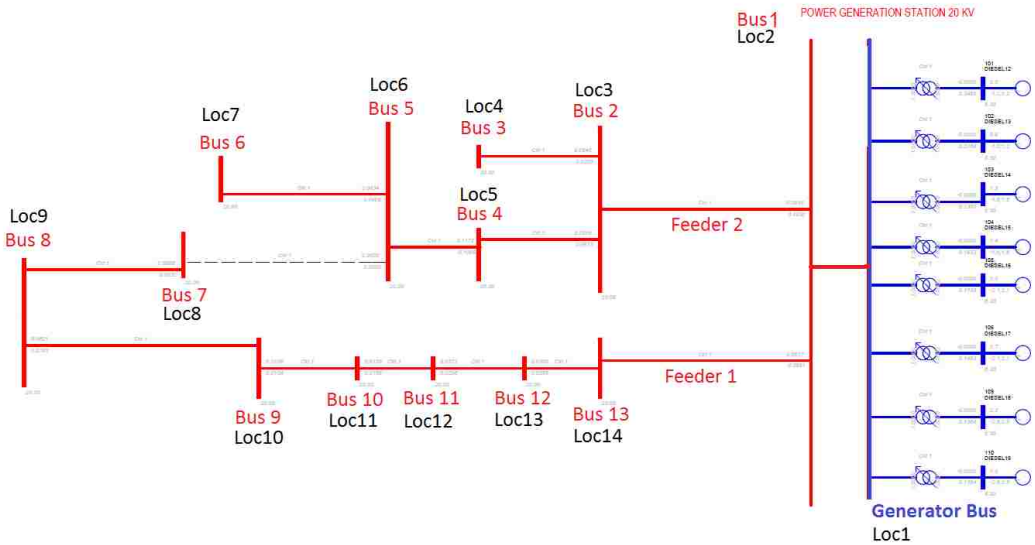

Figure 4.2: One Line Diagram for 14-Nodes configuration

Table 4.2: Generator Reactances Table

Generator No.	Xpu	Sbase, MVA	Vbase, kV
12	0.237	2	6.3
13	0.25	2	6.3
14	0.21	2.7	6.3
15	0.21	2.7	6.3
16	0.223	3.55	6.3
17	0.223	3.55	6.3
18	0.2	4.4	6.3
19	0.2	4.4	6.3

$$Xpu, new = \frac{Sbase, new}{Sbase, old} X Xpu, old$$

where,

Xpu, old = Per unit reactance of generators in their respective Sbase as given in

Table 5.2

Sbase,old = Base power of generators provided

Sbase,new = Base power of system (10MVA)

Xpu, new = Per unit reactance of generators in system power base (10 MVA)

The new equivalent reactance between the generator bus and Bus 1 is calculated by using the parallel combination of 8 different sets of generator and transformer reactances. But before solving the combination, first reactances of all generators had to be converted into a same base system, that is S_{base} of 10 MVA. For this, using the above expression new reactances of generators in common system power base were calculated and subsequently added to those of the transformers connecting them to Bus 2 bus (loc2). Those of transformers were provided with the same base system of 10 MVA. The calculation was done using an Excel spreadsheet and as shown in Table 4.3.

Table 4.3: Table of per unit reactance of Generators in system base (10 MVA)

Generator No.	Xpu, old	Sbase, old	Sbase, new	Xpu, new
12	0.237	2	10	1.185
13	0.25	2	10	1.25
14	0.21	2.7	10	0.777778
15	0.21	2.7	10	0.777778
16	0.223	3.55	10	0.628169
17	0.223	3.55	10	0.628169
18	0.2	4.4	10	0.454545
19	0.2	4.4	10	0.454545

After converting the reactances of transformers and generators into common base of S_{base} of 10 MVA, parallel combination of 8 different branches was carried out. The reactance of each branch is the sum of reactances of its generator and transformer.

$$\frac{1}{Xpu, total} = \frac{1}{Xpu1} + \frac{1}{Xpu2} + \frac{1}{Xpu3} + \frac{1}{Xpu4} + \frac{1}{Xpu5} + \frac{1}{Xpu6} + \frac{1}{Xpu6} + \frac{1}{Xpu7} + \frac{1}{Xpu8}$$

The result came out to be 0.1082 pu. Hence, the new table of 14-Node config-

Table 4.4: Table of reactances between Generator Bus (loc1) and Bus 2 (loc2)

Xpu, lebel	Xpu, generator	Xpu, Transformer	Xpu, total
Xpu1	1.185	0.3465	1.5315
Xpu2	1.25	0.2785	1.5285
Xpu3	0.777778	0.236	1.013778
Xpu4	0.777778	0.19333	0.971108
Xpu5	0.628169	0.17361	0.801779
Xpu6	0.628169	0.14925	0.777419
Xpu7	0.454545	0.13636	0.590905
Xpu8	0.454545	0.13636	0.590905

uration with updated branch parameters and location numbers for DER-CAM was like in Table 4.4.

Table 4.5: 14-node Branch Data

Loc No.	Bus Name	Loc No.	Bus Name	R (pu)	X (pu)
1	GENERATOR BUS	2	Bus 2	0	0.108207
2	Bus 1	3	Bus 2	0.06152	0.09304
2	Bus 1	14	Bus 13	0.08268	0.06611
3	Bus 2	4	Bus 3	0.054	0.022
3	Bus 2	5	Bus 4	0.05495	0.05133
5	Bus 4	6	Bus 5	0.11724	0.10952
6	Bus 5	7	Bus 6	0.05338	0.04987
6	Bus 5	8	Bus 7	0.00204	0.00201
8	Bus 7	9	Bus 8	0.09982	0.09325
9	Bus 8	10	Bus 9	0.08208	0.07667
10	Bus 9	11	Bus 10	0.01563	0.01042
11	Bus 10	12	Bus 11	0.01687	0.01663
12	Bus 11	13	Bus 12	0.03725	0.02979
13	Bus 12	14	Bus 13	0.038	0.02676

After calculating the branch parameters between Generator Bus (loc1) and Bus 2 (loc2) branch capacity was estimated. The branch capacity was assumed to be 50 MVA to be in a safe side and length as 0. Information about branch capacities and lengths were supplied to DER-CAM in the form of upper triangular matrices which were as shown in Table 4.6 and Table 4.7.

Table 4.6: Branch Capacity (MVA) Matrix for 14-Nodes

	loc1	loc2	loc3	loc4	loc5	loc6	loc7	loc8	loc9	loc10	loc11	loc12	loc13	loc 14
loc1	0	50	0	0	0	0	0	0	0	0	0	0	0	0
loc2	0	0	11.6	0	0	0	0	0	0	0	0	0	0	7
loc3	0	0	0	4.7	8.7	0	0	0	0	0	0	0	0	0
loc4	0	0	0	0	0	0	0	0	0	0	0	0	0	0
loc5	0	0	0	0	0	8.7	0	0	0	0	0	0	0	0
loc6	0	0	0	0	0	0	8.7	8.7	0	0	0	0	0	0
loc7	0	0	0	0	0	0	0	0	0	0	0	0	0	0
loc8	0	0	0	0	0	0	0	0	8.7	0	0	0	0	0
loc9	0	0	0	0	0	0	0	0	0	8.7	0	0	0	0
loc10	0	0	0	0	0	0	0	0	0	0	6.8	0	0	0
loc11	0	0	0	0	0	0	0	0	0	0	0	8.7	0	0
loc12	0	0	0	0	0	0	0	0	0	0	0	0	7	0
loc13	0	0	0	0	0	0	0	0	0	0	0	0	0	6.7
loc14	0	0	0	0	0	0	0	0	0	0	0	0	0	0

Table 4.7: Length (m) Matrix for 14-Nodes

	loc1	loc2	loc3	loc4	loc5	loc6	loc7	loc8	loc9	loc10	loc11	loc12	loc13	loc14
loc1	0	0	0	0	0	0	0	0	0	0	0	0	0	0
loc2	0	0	9700	0	0	0	0	0	0	0	0	0	0	6300
loc3	0	0	0	3200	5200	0	0	0	0	0	0	0	0	0
loc4	0	0	0	0	0	0	0	0	0	0	0	0	0	0
loc5	0	0	0	0	0	11100	0	0	0	0	0	0	0	0
loc6	0	0	0	0	0	0	5100	200	0	0	0	0	0	0
loc7	0	0	0	0	0	0	0	0	0	0	0	0	0	0
loc8	0	0	0	0	0	0	0	0	9500	0	0	0	0	0
loc9	0	0	0	0	0	0	0	0	0	7800	0	0	0	0
loc10	0	0	0	0	0	0	0	0	0	0	1000	0	0	0
loc11	0	0	0	0	0	0	0	0	0	0	0	1700	0	0
loc12	0	0	0	0	0	0	0	0	0	0	0	0	2800	0
loc13	0	0	0	0	0	0	0	0	0	0	0	0	0	2600
loc14	0	0	0	0	0	0	0	0	0	0	0	0	0	0

4.4 Formation of Admittance and Impedance Matrix

Formation of admittance and impedance matrix needed the branch connections and their line parameters resistance (R) and reactance (X) in per unit which have been formulated as above. However, in our calculation of Y/Z matrix, it was assumed that the effect of charging capacitance (B) and shunt admittance were negligible. This assumption was used in formulating the approximated voltages equations used in DER-CAM as discussed earlier [7].

The Admittance (Ybus) matrix was calculated using a matlab program using only the admittances between the buses and it came out to be 14×14 as expected. However, impedance matrix (Zbus) was not simply calculating by inversing the Ybus. As explained in the information section above, the power flow equations implemented

in DER-CAM to approximate the voltages of different nodes linearly did not require the impedances of lines connected to slack bus (loc1) [7]. Hence, the first row and column of the admittance matrix were removed and inverse of the remaining 13×13 truncated matrix is calculated. The resultant matrix was then made 14×14 by adding a row and a column upfront with all zeros on them. That was also helpful because the Y matrix was not readily invertible [7] but could be done by eliminating the slack bus connections as described above. The Ybus and Zbus were then broken down into their real and imaginary parts as in Table 4.8, Table 4.9, Table 4.10 and Table 4.11 as required by DER-CAM.

Table 4.8: Real Admittance Matrix (Ybus real) for 14-Nodes

	loc1	loc2	loc3	loc4	loc5	loc6	loc7	loc8	loc9	loc10	loc11	loc12	loc13	loc 14
loc1	0	0	0	0	0	0	0	0	0	0	0	0	0	0
loc2	0	12.3227	-4.9448	0	0	0	0	0	0	0	0	0	0	-7.3778
loc3	0	-4.9448	30.5455	-15.8823	-9.7183	0	0	0	0	0	0	0	0	0
loc4	0	0	-15.8823	15.8823	0	0	0	0	0	0	0	0	0	0
loc5	0	0	-9.7183	0	14.2731	-4.5548	0	0	0	0	0	0	0	0
loc6	0	0	0	0	-4.5548	263.2866	-10.0029	-248.729	0	0	0	0	0	0
loc7	0	0	0	0	0	-10.0029	10.0029	0	0	0	0	0	0	0
loc8	0	0	0	0	0	-248.729	0	254.0784	-5.3495	-6.5063	0	0	0	0
loc9	0	0	0	0	0	0	0	-5.3495	11.8558	-6.5063	-44.2935	0	0	0
loc10	0	0	0	0	0	0	0	0	-6.5063	50.7998	74.3565	-30.063	0	0
loc11	0	0	0	0	0	0	0	0	0	-44.2935	-30.063	46.4366	-16.3735	0
loc12	0	0	0	0	0	0	0	0	0	0	0	-16.3735	33.9653	-17.5917
loc13	0	0	0	0	0	0	0	0	0	0	0	0	-17.5917	24.9696
loc14	0	-7.3778	0	0	0	0	0	0	0	0	0	0		

Table 4.9: Imaginary Admittance Matrix (Ybus imag) for 14-Nodes

	loc1	loc2	loc3	loc4	loc5	loc6	loc7	loc8	loc9	loc10	loc11	loc12	loc13	loc 14
loc1	-31.5159	31.5159	0	0	0	0	0	0	0	0	0	0	0	0
loc2	31.5159	-44.8935	7.4784	0	0	0	-9.3451	0	4.9974	0	0	0	0	5.8992
loc3	0	7.4784	-23.027	6.4705	9.078	0	0	0	0	0	0	0	0	0
loc4	0	0	6.4705	-6.4705	0	0	0	0	0	0	0	0	0	0
loc5	0	0	9.078	0	-13.3329	4.2548	0	0	0	0	0	0	0	0
loc6	0	0	0	0	4.2548	-258.671	9.3451	245.0711	0	0	0	0	0	0
loc7	0	0	0	0	0	9.3451	-9.3451	0	0	0	0	0	0	0
loc8	0	0	0	0	0	245.0711	0	-250.069	4.9974	0	0	0	0	0
loc9	0	0	0	0	0	0	0	4.9974	-11.0749	6.0774	0	0	0	0
loc10	0	0	0	0	0	0	0	0	6.0774	-35.6064	29.529	0	0	0
loc11	0	0	0	0	0	0	0	0	0	29.529	-59.1643	29.6353	0	0
loc12	0	0	0	0	0	0	0	0	0	0	29.6353	-42.7298	13.0944	0
loc13	0	0	0	0	0	0	0	0	0	0	0	13.0944	-25.4827	12.3883
loc14	0	5.8992	0	0	0	0	0	0	0	0	0	0	12.3883	-18.2875

Table 4.10: Real Impedance Matrix (Zbus real) for 14-Nodes

	loc1	loc2	loc3	loc4	loc5	loc6	loc7	loc8	loc9	loc10	loc11	loc12	loc13	loc 14
loc1	0	0	0	0	0	0	0	0	0	0	0	0	0	0
loc2	0	0	0	0	0	0	0	0	0	0	0	0	0	0
loc3	0	0	0.0563	0.0563	0.0507	0.0388	0.0388	0.0386	0.0285	0.0201	0.0184	0.0167	0.0128	0.0087
loc4	0	0	0.0563	0.1103	0.0507	0.0388	0.0388	0.0386	0.0285	0.0201	0.0184	0.0167	0.0128	0.0087
loc5	0	0	0.0507	0.0507	0.0951	0.0726	0.0726	0.0722	0.0531	0.0373	0.0342	0.031	0.0237	0.0161
loc6	0	0	0.0388	0.0388	0.0726	0.1448	0.1448	0.144	0.1056	0.074	0.0679	0.0614	0.0469	0.0321
loc7	0	0	0.0388	0.0388	0.0726	0.1448	0.1981	0.144	0.1056	0.074	0.0679	0.0614	0.0469	0.0321
loc8	0	0	0.0386	0.0386	0.0722	0.144	0.144	0.1452	0.1065	0.0746	0.0685	0.0619	0.0473	0.0323
loc9	0	0	0.0285	0.0285	0.0531	0.1056	0.1056	0.1065	0.1512	0.1059	0.0971	0.0878	0.0671	0.0459
loc10	0	0	0.0201	0.0201	0.0373	0.074	0.074	0.0746	0.1059	0.1316	0.1207	0.1091	0.0834	0.0571
loc11	0	0	0.0184	0.0184	0.0342	0.0679	0.0679	0.0685	0.0971	0.1207	0.1251	0.1131	0.0864	0.0591
loc12	0	0	0.0167	0.0167	0.031	0.0614	0.0614	0.0619	0.0878	0.1091	0.1131	0.1175	0.0898	0.0614
loc13	0	0	0.0128	0.0128	0.0237	0.0469	0.0469	0.0473	0.0671	0.0834	0.0864	0.0898	0.0971	0.0664
loc14	0	0	0.0087	0.0087	0.0161	0.0321	0.0321	0.0323	0.0459	0.0571	0.0591	0.0614	0.0664	0.0715

Table 4.11: Imaginary Impedance Matrix (Zbus imag) for 14-Nodes

	loc1	loc2	loc3	loc4	loc5	loc6	loc7	loc8	loc9	loc10	loc11	loc12	loc13	loc 14
loc1	0	0	0	0	0	0	0	0	0	0	0	0	0	0
loc2	0	0.0317	0.0317	0.0317	0.0317	0.0317	0.0317	0.0317	0.0317	0.0317	0.0317	0.0317	0.0317	0.0317
loc3	0	0.0317	0.1108	0.1108	0.1025	0.0847	0.0847	0.0844	0.0693	0.0569	0.055	0.0524	0.0474	0.0428
loc4	0	0.0317	0.1108	0.1328	0.1025	0.0847	0.0847	0.0844	0.0693	0.0569	0.055	0.0524	0.0474	0.0428
loc5	0	0.0317	0.1025	0.1025	0.1409	0.1134	0.1134	0.1129	0.0895	0.0702	0.0674	0.0633	0.0556	0.0486
loc6	0	0.0317	0.0847	0.0847	0.1134	0.1745	0.1745	0.1737	0.1325	0.0986	0.0939	0.0866	0.0733	0.0612
loc7	0	0.0317	0.0847	0.0847	0.1134	0.1745	0.2244	0.1737	0.1325	0.0986	0.0939	0.0866	0.0733	0.0612
loc8	0	0.0317	0.0844	0.0844	0.1129	0.1737	0.1737	0.1748	0.1333	0.0992	0.0944	0.087	0.0736	0.0614
loc9	0	0.0317	0.0693	0.0693	0.0895	0.1325	0.1325	0.1333	0.1699	0.1234	0.1169	0.1069	0.0886	0.0721
loc10	0	0.0317	0.0569	0.0569	0.0702	0.0986	0.0986	0.0992	0.1234	0.1433	0.1355	0.1232	0.101	0.0809
loc11	0	0.0317	0.055	0.055	0.0674	0.0939	0.0939	0.0944	0.1169	0.1355	0.1379	0.1253	0.1026	0.0821
loc12	0	0.0317	0.0524	0.0524	0.0633	0.0866	0.0866	0.087	0.1069	0.1232	0.1253	0.1289	0.1053	0.084
loc13	0	0.0317	0.0474	0.0474	0.0556	0.0733	0.0733	0.0736	0.0886	0.101	0.1026	0.1053	0.11	0.0874
loc14	0	0.0317	0.0428	0.0428	0.0486	0.0612	0.0612	0.0614	0.0721	0.0809	0.0821	0.084	0.0874	0.0903

4.5 Generation characterization

DER-CAM needs various information about specification of all generators for power flow studies as well as financial analysis and optimization, which were as follows:

- Maximum Power in kW
- Generator Lifetime in years
- Capital cost of each unit
- Fix operation and maintenance cost
- Variable operation and maintenance cost
- Sprinting Capacity and hours
- Efficiency

Out of these information, the generator ratings and minimum loads were provided to us as in the following Table 4.12. The minimum loading information was converted into in terms of fraction as required by DER-CAM. Similarly, the sprint capacity was

Table 4.12: Minimum Loadings of generators

Genset	unit power kW	Min. load (kW)	Min. load
12 & 13	1400	840	0.6
14 & 15	1840	956.8	0.52
16 & 17	2510	1430.7	0.57
18 & 19	3100	1705	0.55

estimated to be just bigger than the rated capacity. Those generators were assumed to be able to run for 48 hours in sprint capacity as in the following Table 4.13. DER-CAM had provisions for both fixed and variable efficiencies of generators but a fixed value was used for simplicity. As we were provided with hourly fuel costs and fuel prices for each generators. Using the hourly thermal energy calculated from calorific value of fuel, efficiency for each generators was calculated from the hourly ration of

electric output and thermal input as shown in Figure 4.3. Average of these efficiencies were used in DER-CAM and these values suggested that the larger generators had better efficiencies as expected.

Table 4.13: Generator Sprint Capacities and Efficiencies

Diesel Genset	unit power kW	Sprint Capacity kW	Sprint hours	Efficiency
12 & 13	1400	1600	48	0.34
14 & 15	1840	2000	48	0.36
16 & 17	2510	2700	48	0.37
18 & 19	3100	3500	48	0.38

As for the generator lifetime, 20 years was selected. Financial data such as capital costs, fix and variable operation and maintenance costs were discussed in Chapter 7 .

4.6 Loads

DER-CAM has its own format of load data to be plugged in for some specific load types: peak, week and weekend. The current version of the DER-CAM lets us use the various types of loads as follows:

- Electricity only
- Cooling
- Refrigeration
- Space-heating
- Water-heating
- Natural gas only

All of these loads were to be entered in a specific format. It basically contained the 24 hourly data for each month in terms of peak, week and weekend. However, we

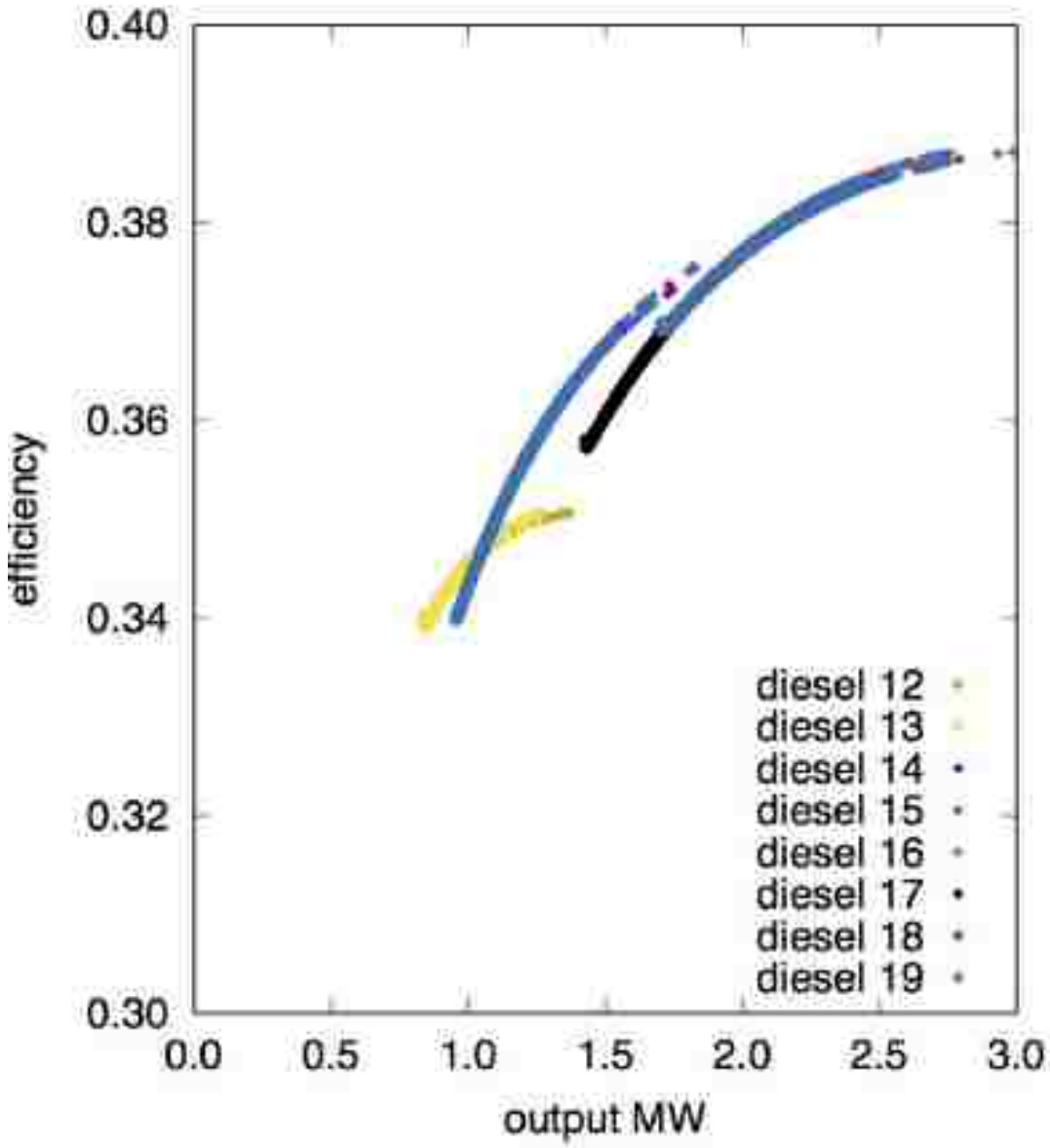

Figure 4.3: Efficiency of generators

were only concerned with modeling and optimizing the microgrid in terms of electric power analysis. Hence, we looked into modeling the electrical (Electricity only) loads

and all of the other load types were set to zero.

We were provided with historical hourly loads for a whole year which had to be converted into specific load format as DER-CAM required. DER-CAM required all three types of load at every months and hours. This was done on a excel spread worksheet what would compute the loads for each months and hours for all load types (week, weekend and peak) from the hourly load profile in kilowatts.

With the calculations in excel file, the load data is formatted as required in DER-CAM for all the load centers of our network. Figure 4.4, 4,5 and 4.6 represent peak, week and weekend profile of loads at Bus 6 (loc7) which is considered as the biggest load center as well. The x-axis refers to the 24 hours in a day and y-axis load in kW.

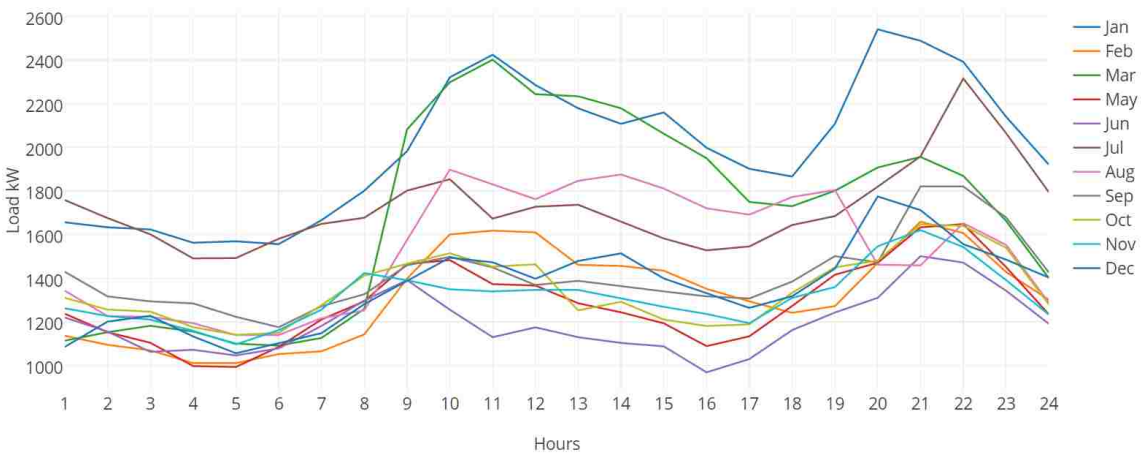

Figure 4.4: Peak hourly load profile for each months of San Sebastian

The figures showed that load values at the bus were higher at the month of January. It was also the month where EPRI and the utility company reported to have the maximum load demand. Since the island's biggest industry was tourism and January would be the month where higher number of tourists come to visit, the microgrid having the maximum load was justified. This also supported the fact that the total load was maximum at Jan 11 AM. The generalized slope of the curves also

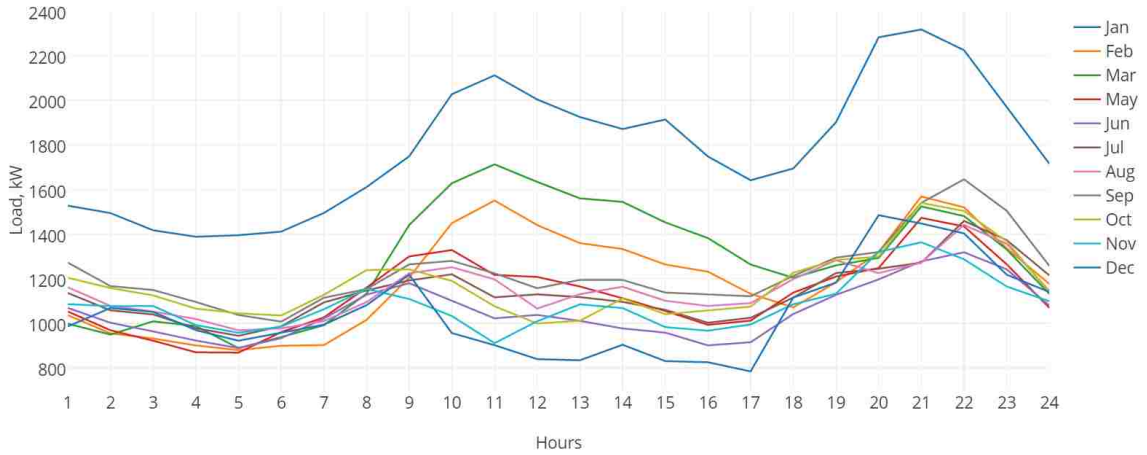

Figure 4.5: Weekdays hourly load profile for each months of San Sebastian

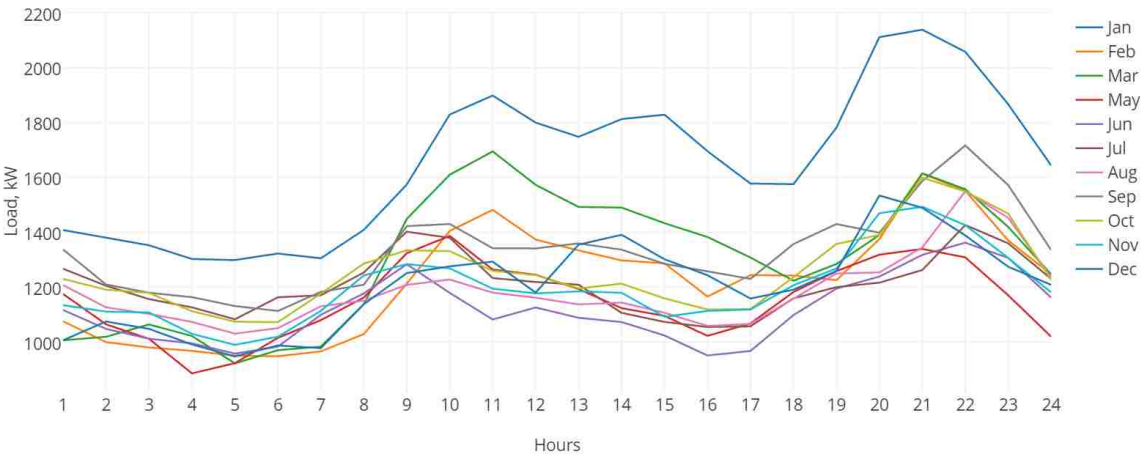

Figure 4.6: Weekend hourly load profile for each months of San Sebastian

suggested that load demand is higher at morning hours from 9 AM to 11 AM and evening hours from 7 PM to 22 PM.

Chapter 5

Power Flow and Benchmarking with PSS/E

The purpose of this thesis project- integration of optimized Distributed Energy Resources- was only carried out after the results of power flow in DER-CAM were verified. For this purpose, the existing microgrid was simulated in a power flow simulation tool PSSE and the model and results were provided to us for the verification in DER-CAM. The case to run power flow with the existing energy resource technologies and distribution (that is excluding the Distributed Energy Resources to be integrated) was referred as Base case. If results of power flow studies of the Base case from DER-CAM and the simulated ones from PSSE would be reasonably comparable, then the modeling of microgrid and results of power flow in DER-CAM would be accepted. For this specific purpose, the following results were compared between DER-CAM and PSSE:

- Voltages at different buses
- Distribution loss

For the comparison, the Base case was run in DER-CAM with the information from above modeling section and different settings which were discussed below.

5.1 DER-CAM settings

Apart from the information for the network characteristics and specifications, DER-CAM required other settings and conditions to be specified by the users for customized runs.

Iteration settings include the options to control the iterations of equations involved in the study. Most of these settings were used as they were provided already on the tool. DER-CAM was allowed to print the solver status on the results for convenient runs. This setting prove to be very useful during the times of debugging and testing. Limit for the number of iterations to be allowed for equations was set at 5000000. This was the value provided already on the program. Similarly, the time limit for the solver in the CPU time (seconds) was kept at 360000 as was before.

The value for relative termination criterion was run mostly at 0.2%. It was basically the tolerance level for the results and is perceived as the error tolerance of results to be approximated by DER-CAM. During the initial phases of the work, it was kept at a really high value to ensure that the code runs and solutions were feasible. Sometimes it was even set at maximum allowed of 10%- for the sake of faster execution during the debugging and troubleshooting stages.

5.2 Parameters settings

Parameter settings were the options to set up the initial parameters of the equations involved in DER-CAM. DER-CAM required us to set the voltage of the slack bus

and it was set at 1.04 pu as in PSSE.

Base values of the per unit system was one of the most significant aspect in running the power flow including that in DER-CAM. The base value of Power was set at 10000 in kVA and that of voltage at 20 in kV. The base values of power and voltage were used as the same in PSSE to ensure that the per unit values of line parameters (resistances and reactances) would have common reference.

The summary of parameter settings is given in the following Table 5.1.

Table 5.1: Parameter Settings

Slack bus initial Voltage	1.04 pu
Sbase	10000 kVA (10 MVA)
Vbase (Slack Bus)	20 kV

5.3 Network Configuration

The Network configuration data were provided as discussed in the network modeling section. All the 14 locations (14 nodes) of the network were defined and assigned as load bus (PQ bus) except for the location 1 which is set as slack bus. The locations which were neither load bus nor slack bus were still assigned load bus with the load values of zero at all time periods.

The impedance (Zbus) and admittance (Ybus) matrix, cable length matrix, branch capacity matrix were all provided to DER-CAM. The Ybus and Zbus were defined in separate tables of real and imaginary values. The cable length and branch capacity were entered as upper triangular matrices.

5.4 Simulation Parameters

The Simulation Parameters were entered by the user for different options of the Base case cost estimation and modeling. There were several options but those only related to our study were modified and the rest were kept just as they were before. Firstly, the interest rate for the financial analysis was set at 3%.

Base case cost was defined as the total annual energy cost prior to the installation of DERs and one of the major constraint for the DER-CAM operation. The objective of the Base case run was to find the total cost of the energy that can be set as the maximum financial target for the integration of Distributed Energy Resources (DERs). As for the initial Base case run itself, the value of Base case cost was set at infinitely large. After the successful Base case run, a value higher than the total costs of energy from the Base case run was put in Base case cost. The maximum payback period is set at 50 years of time.

Even though Photovoltaics (PV) were not used in Base case run, efficiency of 15.19% was set on the DER-CAM as default PV specifications. Similarly, the information about the solar isolation, ambient temperature and wind speed was also overlooked for the Base case since they were not required at all.

As for the generators, their financial information was updated according with the report from EPRI [9]. The capital cost of the Diesel Generator 12 and 13 were set at €2098/kW whereas for those 14 and 15 at €1587/kW, 16 and 17 at €1143 and 18 and 19 at €865. Fix Operation and Maintenance cost for all of the generators were set at zero and variable cost at the same €0.021/kWh. The summary costs as shown in the following Table 5.2.

Table 5.2: Different costs associated with generators

Gen. Name	Capital Cost(€/kW)	OMFix(€/kW/year)	OMVar(€/kWh)
Diesel 12 & 13	2098	0	0.021
Diesel 14 & 15	1587	0	0.021
Diesel 16 & 17	1143	0	0.021
Diesel 18 & 19	865	0	0.021

5.5 Base Case results using DER-CAM

The configuration of the electrical micrgrid at the island with 14 nodes was ran with DER-CAM using remote logging. The run was expected to give results including the cost analysis of the whole microgrid energy, generator and load dispatches and power flow including the voltage at all nodes, current through each branches. These results served both the purposes of benchmarking with that of PSSE and set the reference for optimization of integration of DERs. The results were categorized and discussed below.

5.5.1 Power Flow results

The Power Flow results given by the DER-CAM were significant for the optimization as they lay out a basis for verification of modeling of the grid. In this section, the power flow results such as the voltages at the nodes and current flowing through branches were studied and analyzed.

Since DER-CAM model the loads in the hourly format for each month and week-load types, the results were also expected to follow in the similar format. For this purpose, the reference for power flow analysis and comparison with PSSE were made on the same load instant as in PSSE. And, the load instant was already taken of the hour at which the load data provided was maximum at which was at Jan 11 AM, peak load.

5.5.2 Voltage and Current Flow

Voltage profile at the different nodes of the network was one of the significant results of the load flow analysis. DER-CAM gave the result of voltages at all locations in per unit for each months, hours and load types (peak, week and weekend). In our current analysis, we had taken into account the voltage values of peak load cases. Figure 5.1 showed the voltage at loc1 (Generator Bus) at peak load. As the voltage at this locations was assumed to be at 1.04 pu, DER-CAM was giving the same voltage level all over the months and hours which was expected.

The voltage profiles as shown in Figure 5.1 to 5.6 suggested that the drops have been up to 0.95 pu. The biggest drops in the voltages occurred at Bus 6 (loc7). That made sense in the way that the further is the location with more loads, the bigger voltage drop is at the place.

Similar to the output voltage results, DER-CAM also gives the monthly and hourly values of current flowing through each branch in the network for all the load types. Some of the results showing current flowing through the transmission lines of the network were shown in Figure 5.7 to Figure 5.11.

In the network, all of the power flowing through across it has flowed through the section connecting between Generator Bus and that at Bus 2. The graph of real current flowing between those two buses showed that the highest current was flowing during the month of January which can be justified with the information that there was very high tourist population in January. It was also inferred that the peak of the loads would be at 11 AM of January.

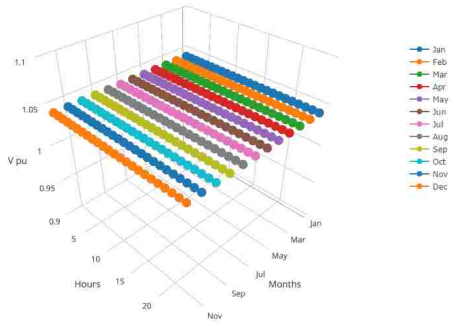

Figure 5.1: Real Voltage (pu) of Generator Bus (loc1) for 14-Nodes

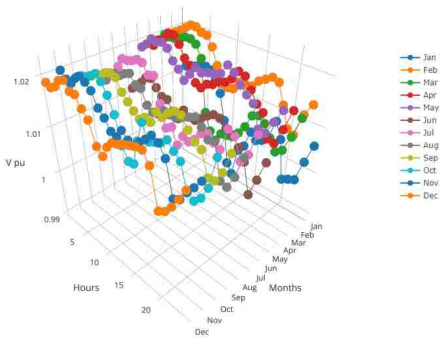

Figure 5.2: Real Voltage (pu) of Bus 4(loc5) for 14-Nodes

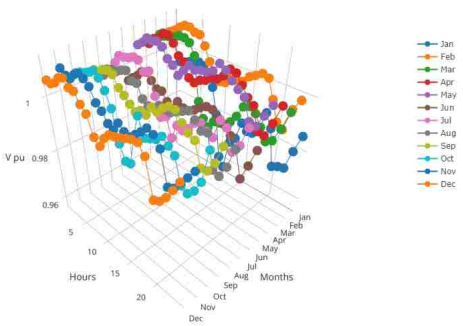

Figure 5.3: Real Voltage (pu) of Bus 5(loc6) for 14-Nodes

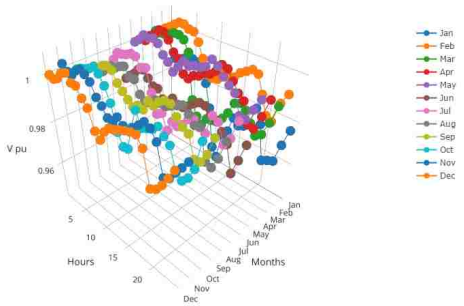

Figure 5.4: Real Voltage (pu) of Bus 6(loc7) for 14-Nodes

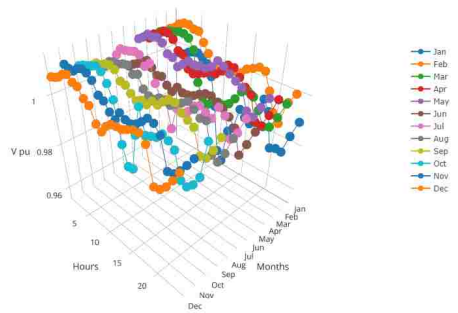

Figure 5.5: Real Voltage (pu) of Bus 7(loc8) for 14-Nodes

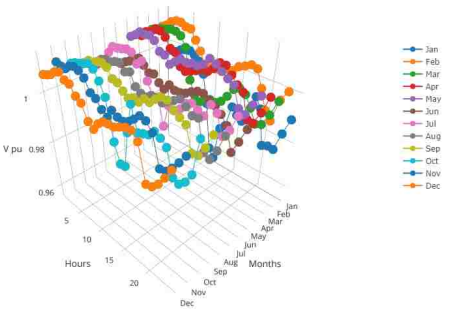

Figure 5.6: Real Voltage (pu) of Bus 8(loc9) for 14-Nodes

5.6 Power Generation, Absorption and Losses

DER-CAM gave results of the power generation by each generators for all months, hours and load types. These results were analyzed to see if the network operation in

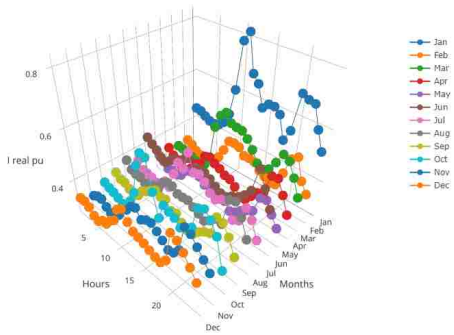

Figure 5.7: Real Current (pu) between loc1 and loc2 for 14-Nodes

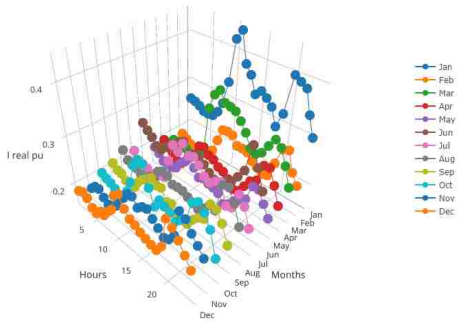

Figure 5.8: Real Current (pu) between loc2 and loc3 for 14-Nodes

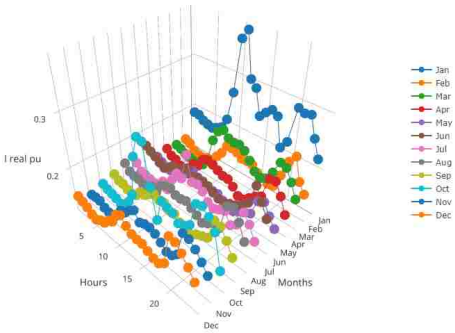

Figure 5.9: Real Current (pu) between loc2 and loc14 for 14-Nodes

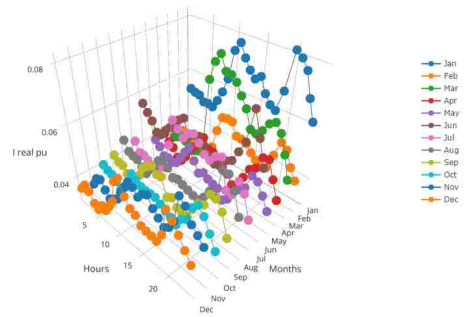

Figure 5.10: Real Current (pu) between loc3 and loc4 for 14-Nodes

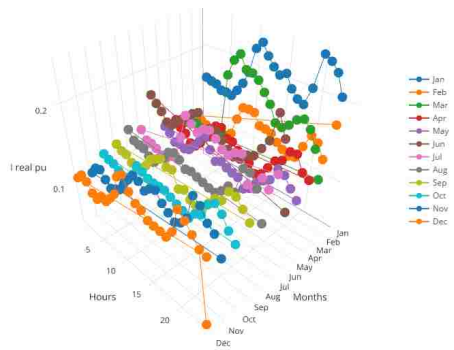

Figure 5.11: Real Current (pu) between loc6 and loc7 for 14-Nodes

terms of power generation and consumption were reasonable.

Four sets of total eight generators were deployed at the generator bus (loc1) that

were kept online during our study. The first two Diesel Generator 12 and 13 were of 1400 kW each, 14 and 15 of 1840 kW each, 16 and 17 of 2510 kW and 18 and 19 of 3100 each. Thus the installed capacity of generators was 17700 kW which was larger than the peak load of 11.7 MW. However, DER-CAM was expected to deploy these generators in such as way that they would be able to meet the load demand with minimum cost of energy and but still operating more than minimum loading conditions of each generators for all hours of operations. Since all of these generators used the same fuel type, they can be expected to get prioritized according to their capital and operation costs and efficiency. Therefore, the power generation of generators was expected to be varying for different hours of operation and might not be generating the power at all too.

These generators were deployed in DER-CAM with four generator types with each type consisting two generators. Hence, their power generation output profile in DER-CAM were observed under their generator types. The generation profile of each generator types for the corresponding peak conditions were shown in Figure 5.12 to Figure 5.15. They had similar generation profiles for week and weekend conditions too.

Based on the above graphs, the Generator sets 18 and 19 were the ones operating to supply most of the load demand. And it was expected because they were the biggest of other generators with highest efficiency. After them, the generator sets 14 and 15 seemed the ones that were operating not much as the earlier ones. Remaining Generator sets 12,13,16 and 17 looked barely operating at all. With these generators operating rarely, installation of energy storage technologies like battery could be solution for supply-demand leveling and hence not to operate some of these generators.

The electrical network dissipates losses through the resistance in transmission lines. Information about this loses were given as output by DER-CAM in the same

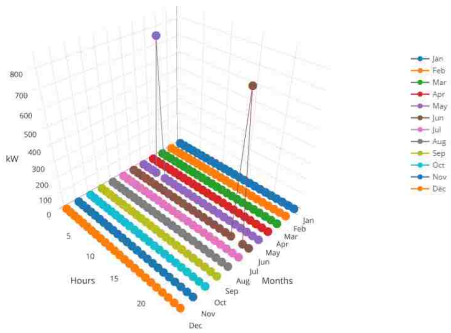

Figure 5.12: Real Power Generation in kW from Generators 12 and 13 for 14-Nodes

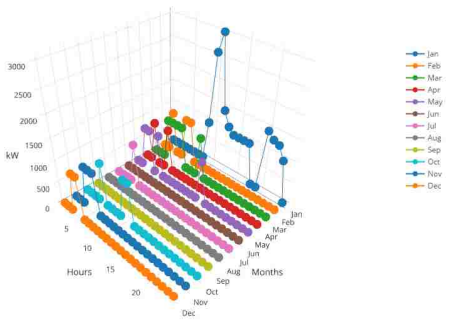

Figure 5.13: Real Power Generation in kW from Generators 14 and 15 for 14-Nodes

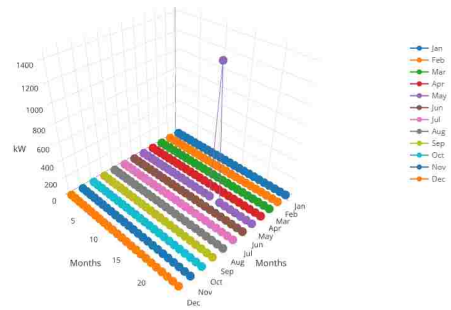

Figure 5.14: Real Power Generation in kW from Generators 16 and 17 for 14-Nodes

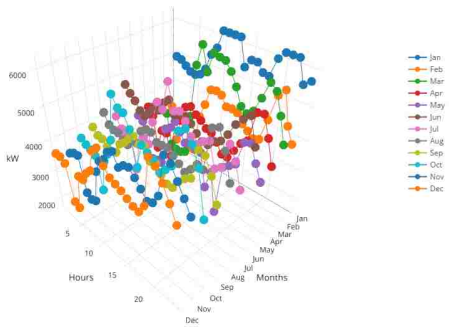

Figure 5.15: Real Power Generation in kW from Generators 18 and 19 for 14-Nodes

load type formats: peak, week and weekend. However, we came to know that DER-CAM sums up the losses as the total real power loss of the entire network rather than showing the individual power loss in each lines. Figures 5.16, 5.17 and 5.18 were the real power loss in pu (with Sbase = 10 MVA) for peak, week and weekend load types.

The above graphs shows that the highest loss in the network occurred at January 11 AM peak time where the loss is 0.066687 pu. The value corresponds to $0.066687 \times Sbase$ (10 MVA) = 0.66687 MW or 666.87 kW of power. It also complied with the fact that the highest loss in the network was expected at the time of the peak demand of the load which also at January 11 AM. Discussions with EPRI and the

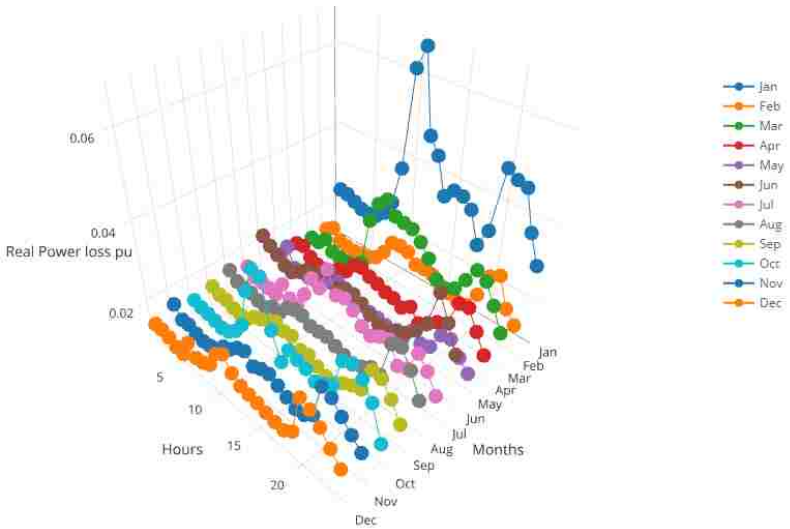

Figure 5.16: Real power loss in pu for 14-Nodes at peak loads

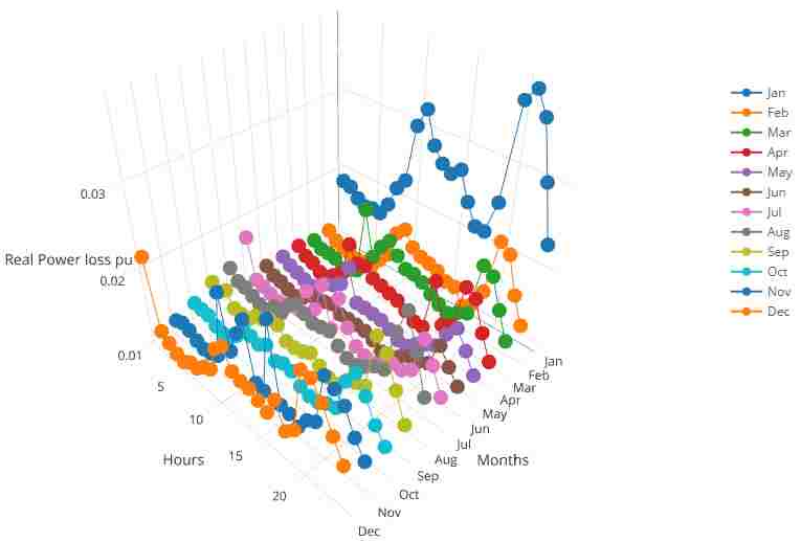

Figure 5.17: Real power loss in pu for 14-Nodes at week loads

utility suggested that the year when the load at feeder lines was provided had the tie-line between Bus 6 (loc7) and Bus 7 (loc8) operating in some cases of peak loads at January which was also a part of reason for the calculated peak loss.

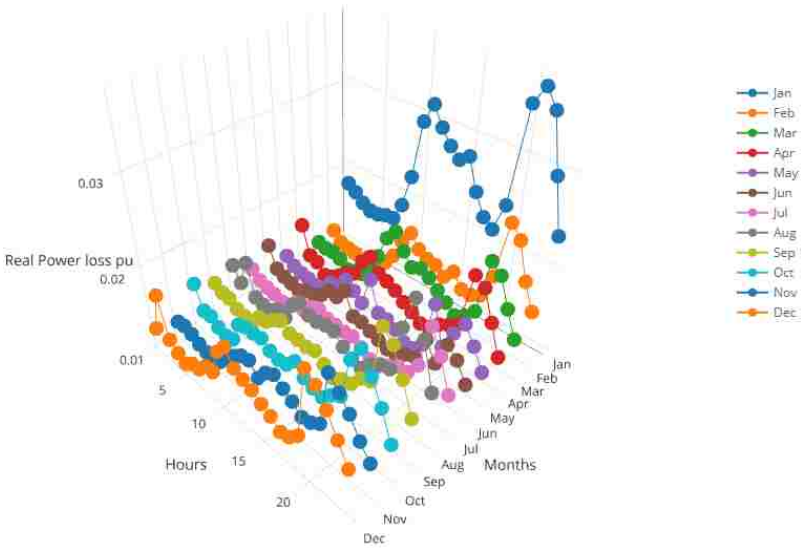

Figure 5.18: Real Power loss in pu for 14-Nodes at weekend loads

5.7 Comparison of Load Flow Results with PSSE

The purpose of the DER-CAM run with 14-nodes configuration was to compare and benchmark the power flow results from DER-CAM with those from PSSE, to make sure that the modeling of microgrid and power flow results from DER-CAM were reasonable. PSSE used the peak load data and ran the power flow simulation at that instant and the results were provided to us in terms of nodal voltages and loses. We looked to compare the nodal voltages and distribution losses between DER-CAM and PSSE.

PSSE simulated the power flow is a single snapshot: only a set of load conditions were given as inputs which was different than the hourly and monthly load profiles for three different load types in DER-CAM. Therefore, for the reference of comparison of the results between PSSE and DER-CAM, we simulated the microgrid in PSSE at maximum loading conditions. And the results in DER-CAM were looked for the maximum load condition which was January 11 AM peak as discussed above.

Table 5.3: Voltage Comparison between DER-CAM and PSSE

Loc no.	Bus Name	Vpu PSSE	Vpu DER-CAM	V diff	V diff %
2	Bus 1	1.0471	1.04	0.0071	0.678063
3	Bus 2	1.0238	1.010816	0.012984	1.268236
4	Bus 3	1.0207	1.006619	0.014081	1.379527
5	Bus 4	1.0096	0.989714	0.019886	1.969708
6	Bus 5	0.9794	0.956869	0.022531	2.300479
7	Bus 6	0.969	0.944442	0.024558	2.534322
8	Bus 7	0.9794	0.956828	0.022572	2.304723
9	Bus 8	1.0245	0.95578	0.06872	6.707667
10	Bus 9	1.0282	0.970917	0.057283	5.57119
11	Bus 10	1.0297	0.97664	0.05306	5.152993
12	Bus 11	1.0315	0.982702	0.048798	4.730761
13	Bus 12	1.0352	0.99621	0.03899	3.766469
14	Bus 13	1.0389	1.010049	0.028851	2.777105

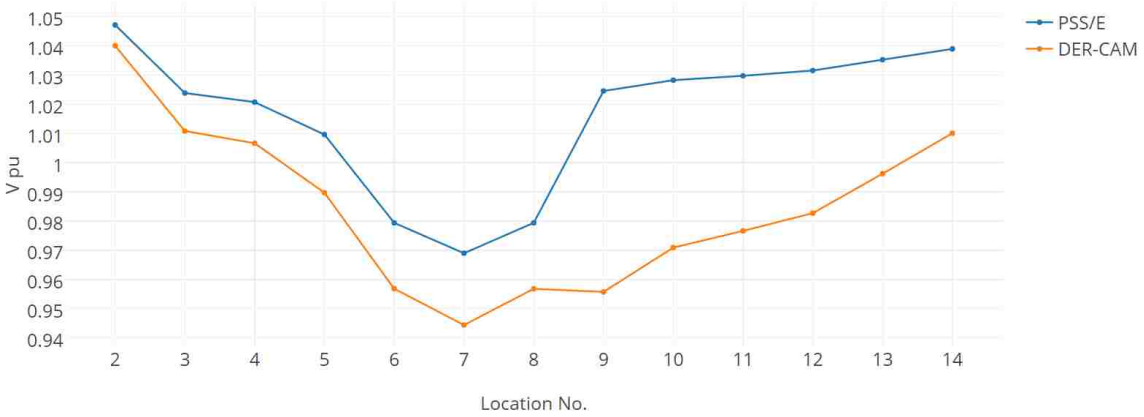

Figure 5.19: Plot of voltage (pu) at different locations from PSSE and DER-CAM

The plots showed that the nodal voltages across the network were within the 10% from generation to the end of feeder lines. Also the voltage differences between that from PSSE and DER-CAM were upto 0.05728 pu which is equivalent to 1.1456 kV in real value. The plot of voltage difference in percentage in Figure 5.19 showed that the highest voltage mismatch was less than 7%.

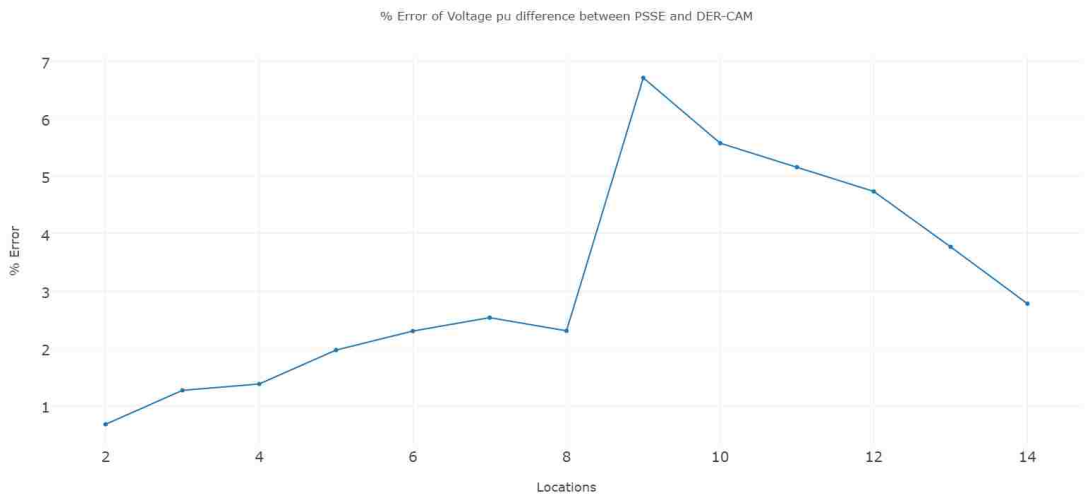

Figure 5.20: Percentage Vpu diff. between PSSE and DER-CAM

Also, the real power loss at the peak loading condition was 666.87 kW (5.7% of peak load 11.7 MW) as found in DER-CAM which was comparable with 8% reported from utilities. The smaller power loss than reported could be because of the fact that we did not take reactive load into account because of DER-CAM limitations. The voltage comparison was said to be reasonable.

Chapter 6

Reconfiguration of the system and Base Case run

Benchmarking with PSSE was done with the network having 14 nodes which however did not represent the real electrical system on the island because it did not take into account the three feeder lines and their loads. Hence, in order to represent the system to as close as possible to real conditions, the three additional nodes were introduced from the Bus 2. The addition of the nodes required the modeling of the system in DER-CAM to reconfigure the whole system.

The new 17-node configuration system was then ran as before and was set as a Base case for the optimization of integration of DERs. The objective value of our optimization function is set as the total energy costs to be minimized by DER-CAM, and the value from the Base case served as a constraint for DERs integration. The optimization was done by enabling the DER-CAM to pick up DERs like PV and electric storage at specified locations by making the total energy costs of energy as low as possible and at the same time meeting the Base case constraint.

6.1 Reconfiguration of the system

Our system earlier had only two feeder lines, Feeder 1 and Feeder 2, with 14 nodes on the network as we omitted three other small feeders Feeder 3, Feeder 4 and Feeder 5. With the addition of these three feeder lines, inputs to the DER-CAM such as a Impedance/Admittance matrices would be different. These data and others like the length, branch capacity and other matrices which were 14×14 earlier would now be 17×17 with the three new nodes. The whole network information provided to the DER-CAM had to be remodeled accordingly to incorporate the three nodes as in Figure 6.1. The three feeder along with their assigned locations were :

- Feeder 3 (loc15)
- Feeder 4 (loc16)
- Feeder 5 (loc17)

The data from EPRI had loads in kW at these nodes as only information about them. The remainder of information such as cable lengths, branch capacities, line resistance and reactance and others had to be estimated. These feeder lines operated at 20 kV voltage like others.

Based on the physical map of the system as shown in Figure 6.1, the lengths of the feeder lines were estimated in comparison with the lengths of Feeder 1 and Feeder 2 whose lenths were already known. They were shown in Table 6.2.

Table 6.1: Lengths of Feeder 3, 4 and 5

From Bus	To Bus	Length(meters)
Bus 2 (loc2)	loc14	2000
Bus 2 (loc2)	loc15	12110
Bus 2 (loc2)	loc17	21650

Line resistance and reactance of these branches were calculated using assumption

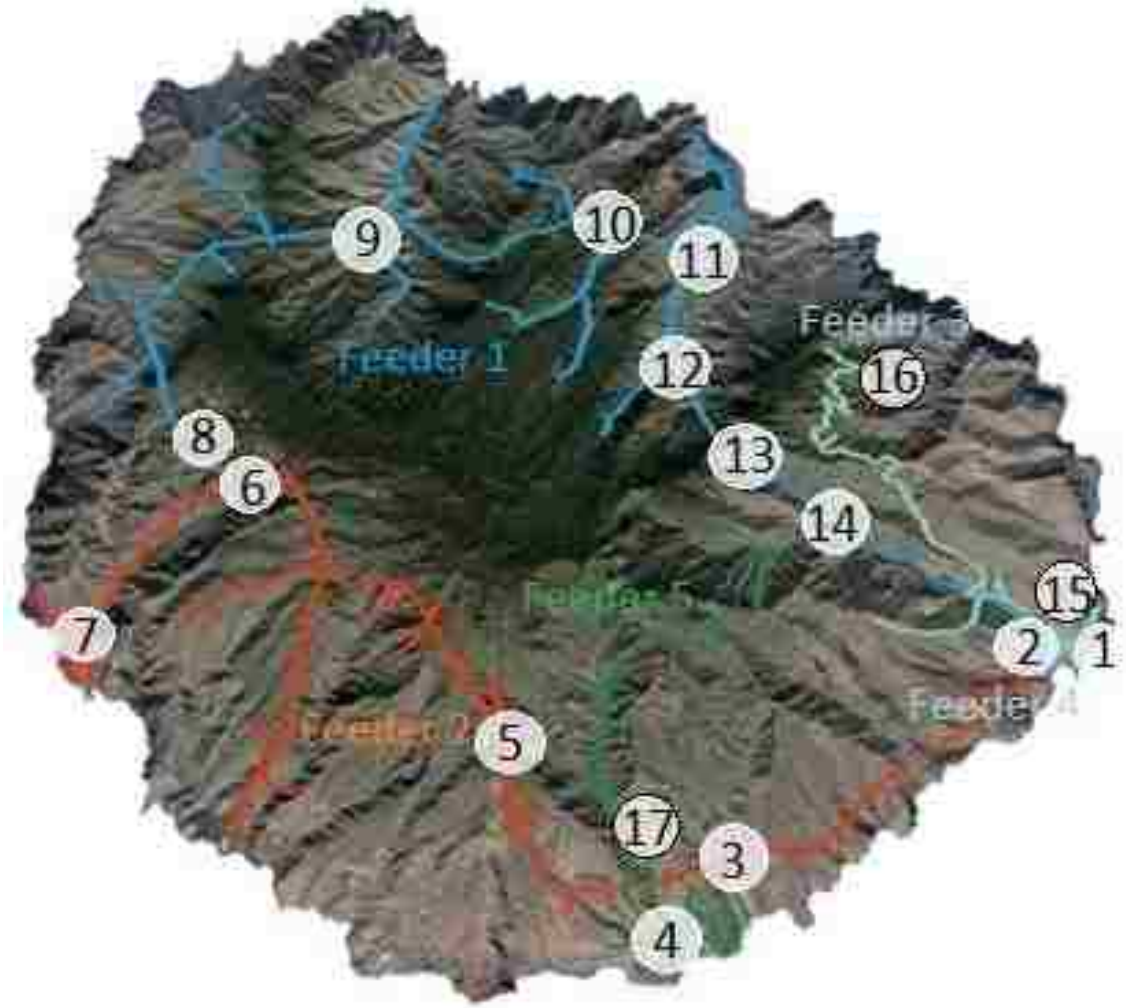

Figure 6.1: La Gomera Island with all feeder lines

of line resistance being 0.1 Ohms per 1 ft. Also it was assumed that the transmission line would have line reactance five times less than the resistance. Using the conversion of 1000 ft = 304.8 meters, the following empirical formula were used for the calculations.

$$Resistance(R), Ohms = \frac{0.1 X length(meters)}{304.8}$$

$$Reactance(X), Ohms = \frac{0.02 X length(meters)}{304.8}$$

These calculated values of resistance and reactance in Ohms were then converted into the per unit values with base power of 10 MVA and base voltage of 20 kV using the following equations.

$$Zbase = \frac{Vbase^2}{Sbase}$$

$$Resistance(R), pu = \frac{R(Ohms)}{Zbase}$$

$$Reactance(X), pu = \frac{X(Ohms)}{Zbase}$$

The new node data table with the three extra nodes is shown in the following Table 6.2. The 'From' and 'To' column refers to the location numbers of connections and 'Length' refers to the length of the sections in meters. This data was then used for the further modeling of the network.

Using the nodal data for 17-nodes configuration, impedance (Zbus) and admittance (Ybus) matrices were formed using the matlab code as in for earlier 14-node system. Also, upper triangular matrices of cable lengths and branch capacities were formed. Cable length matrix had lengths of the cable sections connecting between the various locations in meters and branch capacity matrix consisted of branch capacity of corresponding branch in MVA. The branch capacity for the new feeder branches were assumed to be big-20 MVA- so that DER-CAM did not give infeasible solutions because current ampacity constraints. The new matrices were shown in Table 6.3 to 6.6.

Table 6.2: Nodal data for 17-Nodes configuration

From	To	Length(m)	R, pu	X, pu
1	2	0	0	0.03173
2	3	9700	0.06152	0.09304
2	14	6300	0.08268	0.06611
3	4	3200	0.054	0.022
3	5	5200	0.05495	0.05133
5	6	11100	0.11724	0.10952
6	7	5100	0.05338	0.04987
6	8	200	0.00204	0.00201
8	9	9500	0.09982	0.09325
9	10	7800	0.08208	0.07667
10	11	1000	0.01563	0.01042
11	12	1700	0.01687	0.01663
12	13	2800	0.03725	0.02979
13	14	2600	0.038	0.02676
2	15	2000	0.0164	0.00328
2	16	12110	0.09932	0.01986
2	17	21650	0.17757	0.03551

Table 6.3: Real Admittance matrix (Zbus real)

	loc1	loc2	loc3	loc4	loc5	loc6	loc7	loc8	loc9	loc10	loc11	loc12	loc13	loc14	loc15	loc16	loc17
loc1	0	0	0	0	0	0	0	0	0	0	0	0	0	0	0	0	0
loc2	0	0	0	0	0	0	0	0	0	0	0	0	0	0	0	0	0
loc3	0	0	0.0563	0.0563	0.0507	0.0388	0.0388	0.0386	0.0285	0.0201	0.0184	0.0167	0.0128	0.0087	0	0	0
loc4	0	0	0.0563	0.1103	0.0507	0.0388	0.0388	0.0386	0.0285	0.0201	0.0184	0.0167	0.0128	0.0087	0	0	0
loc5	0	0	0.0507	0.0507	0.0951	0.0726	0.0726	0.0722	0.0531	0.0373	0.0342	0.031	0.0237	0.0161	0	0	0
loc6	0	0	0.0388	0.0388	0.0726	0.1448	0.1448	0.144	0.1056	0.074	0.0679	0.0614	0.0469	0.0321	0	0	0
loc7	0	0	0.0388	0.0388	0.0726	0.1448	0.1981	0.144	0.1056	0.074	0.0679	0.0614	0.0469	0.0321	0	0	0
loc8	0	0	0.0386	0.0386	0.0722	0.144	0.144	0.1452	0.1065	0.0746	0.0685	0.0619	0.0473	0.0323	0	0	0
loc9	0	0	0.0285	0.0285	0.0531	0.1056	0.1056	0.1065	0.1512	0.1059	0.0971	0.0878	0.0671	0.0459	0	0	0
loc10	0	0	0.0201	0.0201	0.0373	0.074	0.074	0.0746	0.1059	0.1316	0.1207	0.1091	0.0834	0.0571	0	0	0
loc11	0	0	0.0184	0.0184	0.0342	0.0679	0.0679	0.0685	0.0971	0.1207	0.1251	0.1131	0.0864	0.0591	0	0	0
loc12	0	0	0.0167	0.0167	0.031	0.0614	0.0614	0.0619	0.0878	0.1091	0.1131	0.1175	0.0898	0.0614	0	0	0
loc13	0	0	0.0128	0.0128	0.0237	0.0469	0.0469	0.0473	0.0671	0.0834	0.0864	0.0898	0.0971	0.0664	0	0	0
loc14	0	0	0.0087	0.0087	0.0161	0.0321	0.0321	0.0323	0.0459	0.0571	0.0591	0.0614	0.0664	0.0715	0	0	0
loc15	0	0	0	0	0	0	0	0	0	0	0	0	0	0	0.0164	0	0
loc16	0	0	0	0	0	0	0	0	0	0	0	0	0	0	0	0.0993	0
loc17	0	0	0	0	0	0	0	0	0	0	0	0	0	0	0	0	0.1775

Table 6.4: Imaginary Admittance matrix (Zbus imag)

	loc1	loc2	loc3	loc4	loc5	loc6	loc7	loc8	loc9	loc10	loc11	loc12	loc13	loc14	loc15	loc16	loc17
loc1	0	0	0	0	0	0	0	0	0	0	0	0	0	0	0	0	0
loc2	0	0.0317	0.0317	0.0317	0.0317	0.0317	0.0317	0.0317	0.0317	0.0317	0.0317	0.0317	0.0317	0.0317	0.0317	0.0317	0.0317
loc3	0	0.0317	0.1108	0.1108	0.1025	0.0847	0.0847	0.0844	0.0693	0.0569	0.055	0.0524	0.0474	0.0428	0.0317	0.0317	0.0317
loc4	0	0.0317	0.1108	0.1328	0.1025	0.0847	0.0847	0.0844	0.0693	0.0569	0.055	0.0524	0.0474	0.0428	0.0317	0.0317	0.0317
loc5	0	0.0317	0.1025	0.1025	0.1409	0.1134	0.1134	0.1129	0.0895	0.0702	0.0674	0.0633	0.0556	0.0486	0.0317	0.0317	0.0317
loc6	0	0.0317	0.0847	0.0847	0.1134	0.1745	0.1745	0.1737	0.1325	0.0986	0.0939	0.0866	0.0733	0.0612	0.0317	0.0317	0.0317
loc7	0	0.0317	0.0847	0.0847	0.1134	0.1745	0.2244	0.1737	0.1325	0.0986	0.0939	0.0866	0.0733	0.0612	0.0317	0.0317	0.0317
loc8	0	0.0317	0.0844	0.0844	0.1129	0.1737	0.1737	0.1748	0.1333	0.0992	0.0944	0.087	0.0736	0.0614	0.0317	0.0317	0.0317
loc9	0	0.0317	0.0693	0.0693	0.0895	0.1325	0.1325	0.1333	0.1699	0.1234	0.1169	0.1069	0.0886	0.0721	0.0317	0.0317	0.0317
loc10	0	0.0317	0.0569	0.0569	0.0702	0.0986	0.0986	0.0992	0.1234	0.1433	0.1355	0.1232	0.101	0.0809	0.0317	0.0317	0.0317
loc11	0	0.0317	0.055	0.055	0.0674	0.0939	0.0939	0.0944	0.1169	0.1355	0.1379	0.1253	0.1026	0.0821	0.0317	0.0317	0.0317
loc12	0	0.0317	0.0524	0.0524	0.0633	0.0866	0.0866	0.087	0.1069	0.1232	0.1253	0.1289	0.1053	0.084	0.0317	0.0317	0.0317
loc13	0	0.0317	0.0474	0.0474	0.0556	0.0733	0.0733	0.0736	0.0886	0.101	0.1026	0.1053	0.11	0.0874	0.0317	0.0317	0.0317
loc14	0	0.0317	0.0428	0.0428	0.0486	0.0612	0.0612	0.0614	0.0721	0.0809	0.0821	0.084	0.0874	0.0903	0.0317	0.0317	0.0317
loc15	0	0.0317	0.0317	0.0317	0.0317	0.0317	0.0317	0.0317	0.0317	0.0317	0.0317	0.0317	0.0317	0.0317	0.035	0.0317	0.0317
loc16	0	0.0317	0.0317	0.0317	0.0317	0.0317	0.0317	0.0317	0.0317	0.0317	0.0317	0.0317	0.0317	0.0317	0.0317	0.0515	0.0317
loc17	0	0.0317	0.0317	0.0317	0.0317	0.0317	0.0317	0.0317	0.0317	0.0317	0.0317	0.0317	0.0317	0.0317	0.0317	0.0317	0.0672

Table 6.5: Length matrix for 17-Nodes

	loc1	loc2	loc3	loc4	loc5	loc6	loc7	loc8	loc9	loc10	loc11	loc12	loc13	loc14	loc15	loc16	loc17
loc1	0	100	0	0	0	0	0	0	0	0	0	0	0	0	0	0	0
loc2	0	0	9700	0	0	0	0	0	0	0	0	0	0	6300	2000	12110	21650
loc3	0	0	0	3200	5200	0	0	0	0	0	0	0	0	0	0	0	0
loc4	0	0	0	0	0	0	0	0	0	0	0	0	0	0	0	0	0
loc5	0	0	0	0	0	11100	0	0	0	0	0	0	0	0	0	0	0
loc6	0	0	0	0	0	0	5100	200	0	0	0	0	0	0	0	0	0
loc7	0	0	0	0	0	0	0	0	9500	0	0	0	0	0	0	0	0
loc8	0	0	0	0	0	0	0	0	0	7800	0	0	0	0	0	0	0
loc9	0	0	0	0	0	0	0	0	0	0	1000	0	0	0	0	0	0
loc10	0	0	0	0	0	0	0	0	0	0	0	1700	0	0	0	0	0
loc11	0	0	0	0	0	0	0	0	0	0	0	0	2800	0	0	0	0
loc12	0	0	0	0	0	0	0	0	0	0	0	0	0	2600	0	0	0
loc13	0	0	0	0	0	0	0	0	0	0	0	0	0	0	0	0	0
loc14	0	0	0	0	0	0	0	0	0	0	0	0	0	0	0	0	0
loc15	0	0	0	0	0	0	0	0	0	0	0	0	0	0	0	0	0
loc16	0	0	0	0	0	0	0	0	0	0	0	0	0	0	0	0	0
loc17	0	0	0	0	0	0	0	0	0	0	0	0	0	0	0	0	0

Table 6.6: Branch Capacity matrix for 17-Nodes

	loc1	loc2	loc3	loc4	loc5	loc6	loc7	loc8	loc9	loc10	loc11	loc12	loc13	loc 14	loc15	loc16	loc17
loc1	0	50	0	0	0	0	0	0	0	0	0	0	0	0	0	0	0
loc2	0	0	11.6	0	0	0	0	0	0	0	0	0	0	7	20	20	20
loc3	0	0	0	4.7	8.7	0	0	0	0	0	0	0	0	0	0	0	0
loc4	0	0	0	0	0	8.7	0	0	0	0	0	0	0	0	0	0	0
loc5	0	0	0	0	0	0	8.7	8.7	0	0	0	0	0	0	0	0	0
loc6	0	0	0	0	0	0	0	0	0	0	0	0	0	0	0	0	0
loc7	0	0	0	0	0	0	0	0	0	0	0	0	0	0	0	0	0
loc8	0	0	0	0	0	0	0	0	8.7	0	0	0	0	0	0	0	0
loc9	0	0	0	0	0	0	0	0	0	8.7	0	0	0	0	0	0	0
loc10	0	0	0	0	0	0	0	0	0	0	6.8	0	0	0	0	0	0
loc11	0	0	0	0	0	0	0	0	0	0	0	8.7	0	0	0	0	0
loc12	0	0	0	0	0	0	0	0	0	0	0	0	7	0	0	0	0
loc13	0	0	0	0	0	0	0	0	0	0	0	0	0	6.7	0	0	0
loc14	0	0	0	0	0	0	0	0	0	0	0	0	0	0	0	0	0
loc15	0	0	0	0	0	0	0	0	0	0	0	0	0	0	0	0	0
loc16	0	0	0	0	0	0	0	0	0	0	0	0	0	0	0	0	0
loc17	0	0	0	0	0	0	0	0	0	0	0	0	0	0	0	0	0

Generator specifications were kept same for the 17-nodes configuration as well. In addition to that, the loads at loc15, loc16 and loc17 were added. The load data at those nodes were provided and processed in the same way to the load format of DER-CAM. The excel file as discussed earlier was used which takes in the hourly load data of whole year and converts into monthly and hourly load profile for three load types: peak, week and weekend.

6.2 Base Case run

The reconfigured electrical system of 17 nodes was run again in DER-CAM without any DERs for the Base case. This study was expected to give the results for the existing running condition and would give the information about the generator dispatches and costs governing the whole system prior to the installation of DERs. The results were then taken as reference for the optimization.

After successful run in DER-CAM, it was found that the addition of the three load feeders and subsequent increase in load resulted increase in distribution losses too. Figure 6.2 graph showing the losses for the peak loads of each months and hours. It was seen that the losses were higher at the months of January because of the high load demand. The new peak loss came out to be 0.0731pu (731 kW). This loss was at the same time- 11 AM of January- when the load was peak (11.7 MW).

One of the significant results, the total costs of energy, was found to be 10.55M. It represented the cost of energy that was calculated after the costs associated from installation of generators to the fuel consumptions and costs associated with delivering the power to the load ends. This Base Cost was going to be the reference cost for the optimized investment case later on.

The costs of fuel was found to be the most significant one, 8.17M out of reported

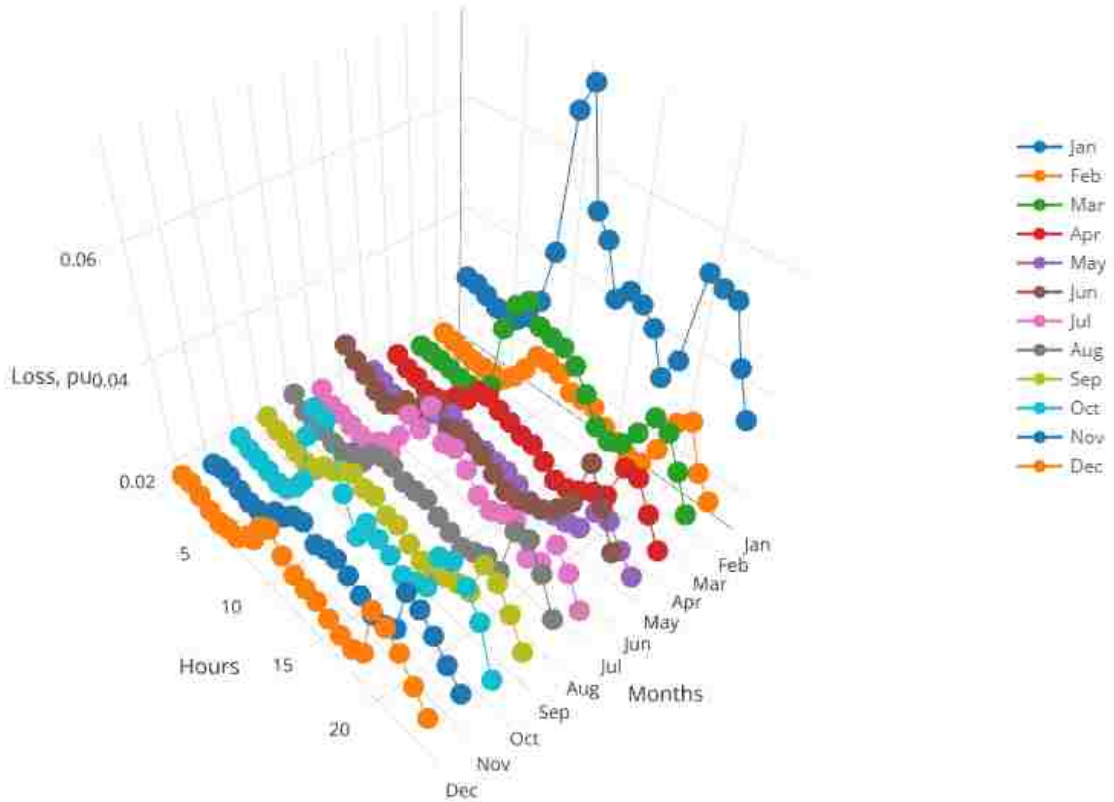

Figure 6.2: Peak Real power loss for Base Case

10.55M costs for energy. It showed that the installation cost of the energy resources was less significant than cost of fuels which would be an encouraging information for the integration of DERs. The total cost of fuel for each month was shown in the following Figure 6.3. The graph shows that the highest fuel consumption was at January where the peak load is, in comparison with other months.

A total of 56.2M kWh of electricity was generated at the location 1 by all generators in a year to supply for the 54.4M kWh of electricity demand. The amount of diesel burnt for this was 149M kWh equivalent. Emission was at around 3.71 X10^7 kgCO_2. Summary of Base Case run of the 17-node system was as in Table 6.7:

Figure 6.3: Total Fuel costs for each month for Base Case

Table 6.7: Summary of Base Case results

Interest Rate	3%
Maximum Payback Period	50 yrs
Peak Distribution Loss	0.0731pu
Total Cost of Energy	10.55M
Toal amount of electricity generated	56.2M kWh
Total Cost of Fuels	8.17M
Total amount of fuel consumed	149M kWh
Emissions	3.71 X10^7 kgCO_2

Chapter 7

Distributed Generation Resources (DERs) and optimization

After the Base Case was run, DER-CAM was allowed to pick up the installation of DERs with optimization at various specified locations. But before this, several parameters including specifications of DERs like their installation costs, performance parameters were required to be set up in DER-CAM. DER-CAM had sizable number of DER options like PV, electric storage, flow battery and wind but looked only at PV and electric storage for this thesis. After defining them, DER-CAM was allowed to select from a set of possible schemes of installations of DERs at different locations.

7.1 Assumptions on DERs

All of these technology schemes fall under continuous investment scheme where DER-CAM was allowed to pick up any non-zero number for their sizes and those numbers were independent with what sizes were available commercially. DER-CAM had many DERs that could be integrated which were given as follows:

- Eelectric Storage
- Heat Storage
- Cold Storage
- Flow Battery Energy
- Flow Battery Power
- Refrigeration
- PV
- Solar Thermal
- Electric Vehicle Storage
- Air Source Heat Pump
- Ground Source Heat Pump
- Wind

However, in our current work we only considered the installations of PV and electric storage. The assumptions regarding PV and electric storage as discussed below.

7.1.1 PV

DER-CAM required financial assumptions regarding the costs such as capital, operation and maintenance and inputs such as solar insolation, ambient temperature.Typical Meteorological Year (TMY) file was used for the closest available location, Las Palmas de Gran Canaria, to find the solar and temperature data. TMY files contain information for the typical month in a number of years usually 30. They can be therefore assumed to be representative of the real weather. DER-CAM required an input of average conditions of each months for 24 hours span. For this,

all hourly data in the TMY file were averaged for each month. Figure 7.1 shows the solar insolation for each hours in all months.

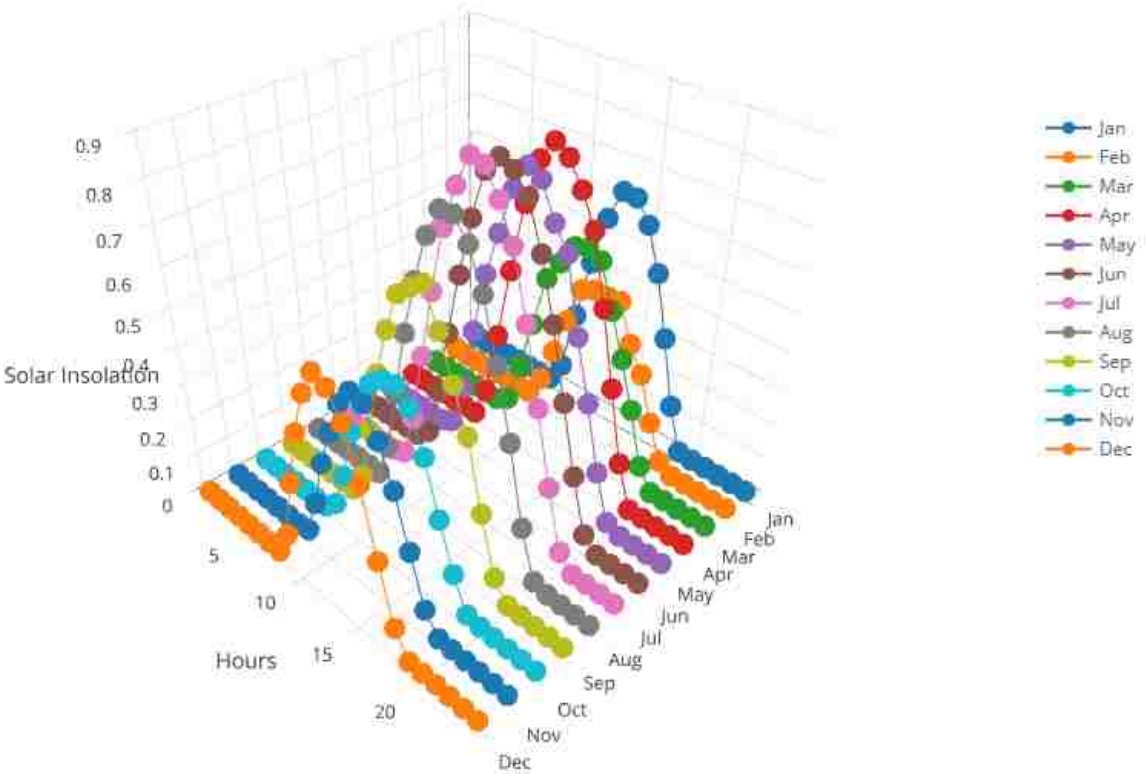

Figure 7.1: Solar Insolation

Another data input required by PV was ambient temperature in degree Celsius. TMY file was used for this information like for the solar insolation. Increase in temperature reduces the efficiency of PV and hence the electricity generation from it is affected. This data was also used by DER-CAM to calculate the electricity generation from PV. Figure 7.2 showed the plot of hourly ambient temperature in Celsius for each months as required in DER-CAM.

DER-CAM used Sanyo H168 PSEL2115 PV cell characteristics as a reference panel [3] to model the efficiency. The maximum efficiency was set at 15.29% and

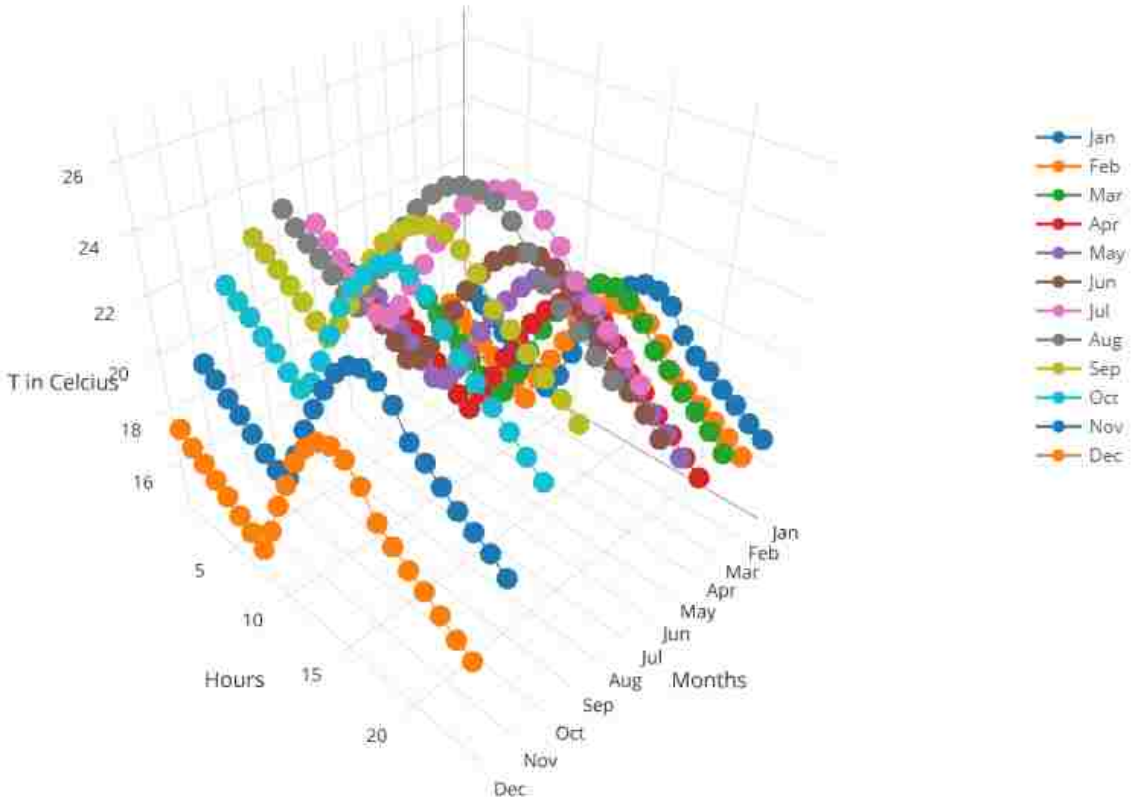

Figure 7.2: Ambient Temperature in ^{0}C

the available space for PV farms (together with Solar Thermal which we did not use though) was 3260000 m^2 (3.26 km^2).

DER-CAM allowed users to specify the cost and performance information regarding the PV. The capital investment cost for PV (Solar PV—Crystalline Utility Scale fixed-tilt design) was found to be €1500 - €1750 in US, and starting 2500 along with investment cost of 2500/kW was set in DER-CAM. This was thought to be the extra price hike due to the transportation inconveniences to island. The lifetime of PV cells were were found to be varying between 25 years - 40 years, so a safe value of 30 years was picked up. Also, variable maintenance cost was set to zero since there was already significant over-estimation of capital costs.

7.1.2 Electric storage

slectric storages also required financial data to be put in DER-CAM. The levelized cost of Lethium-Ion storage for distribution services was between €400 - €789. Taking that into reference, the capital investment cost was set at 500 as fixed and 500/kWh as variable with the battery life time 5 years.

7.1.3 Summary of Financial information about PV and electric storage

Table 7.1: Summary of financial information about PV and electric storage

	PV	electric storage
Fixed Cost €	2500	500
Variable Cost	2500	500
Life time (years)	30	5
Maintenance Cost (E€/kWh)	0	0

7.2 Optimization for different Cases

Optimization in DER-CAM was done with the input data as discussed above and in reference to the total energy cost from Base Case run. In the settings of continuous investment, PV and electric storages were allowed to be optimized by DER-CAM for different location cases. For this the 'forcedinvest' variable was disabled and so was 'forcednumber' so that DER-CAM can pick any non-negative number for PV and electric storage. Since they were defined under continuous investment technologies, their values given by DER-CAM can be anything but negative.

Since the purpose of the study was to see the feasibility and study the different cases of PV and electric storage systems installment at different locations, the opti-

mization runs were divided into several cases defining the schemes of installations of PV only, electric storage only or a combination of both at various locations which were picked up according to suitability. These locations were selected because of their closeness to the big load centers and accessibility. For this, loc4, loc7, loc8 and loc11 were picked up. The first case (Case 0) was assumed to be the Base Case run. The different cases and their results were discussed below.

7.2.1 Case 1: PV only at Bus 6 (loc7)

In this case DER-CAM was allowed to pick up an optimized solution for PV installation at Bus 6 (loc 7). The place was at the farthest end of Feeder 2 on the south western side of the island. And also, since the place was close to the sea transportation of technologies was assumed to be convenient.

DER-CAM picked up 8.85 MV of PV installations on the site of 57898.8 m^2 area. Total of 15020.45 MWh of electricity was generated from the installation of PV. The optimized total costs of energy was reduced to €9.25M, with €1.13M of that being from PV installations. Figure 7.3 shows the hourly PV production for each month.

With the above specified capacity of PV running, electricity generated by the diesel generators decreased to 41112 MWh and the fuel (diesel) consumption reduced to 108769 MWh per year. Emissions was also subsequently reduced to $2.71 \times 10^7 \text{kgCO}_2$.

Figure 7.4 showed the plot of total losses in the network during peak load conditions. From the graph, maximum loss was found to be 0.0545 pu (545kW) during peak load at Jan 20th hour. Installation of PV at Bus 6 have reduced the maximum distribution loss of the network from 731 kW-that was during peak load at Jan 11th hour- by 186kW. Figure 7.5 shows the voltage profile across all the locations (nodes) at peak load condition (Jan 11 AM). It was observed that voltage actually went

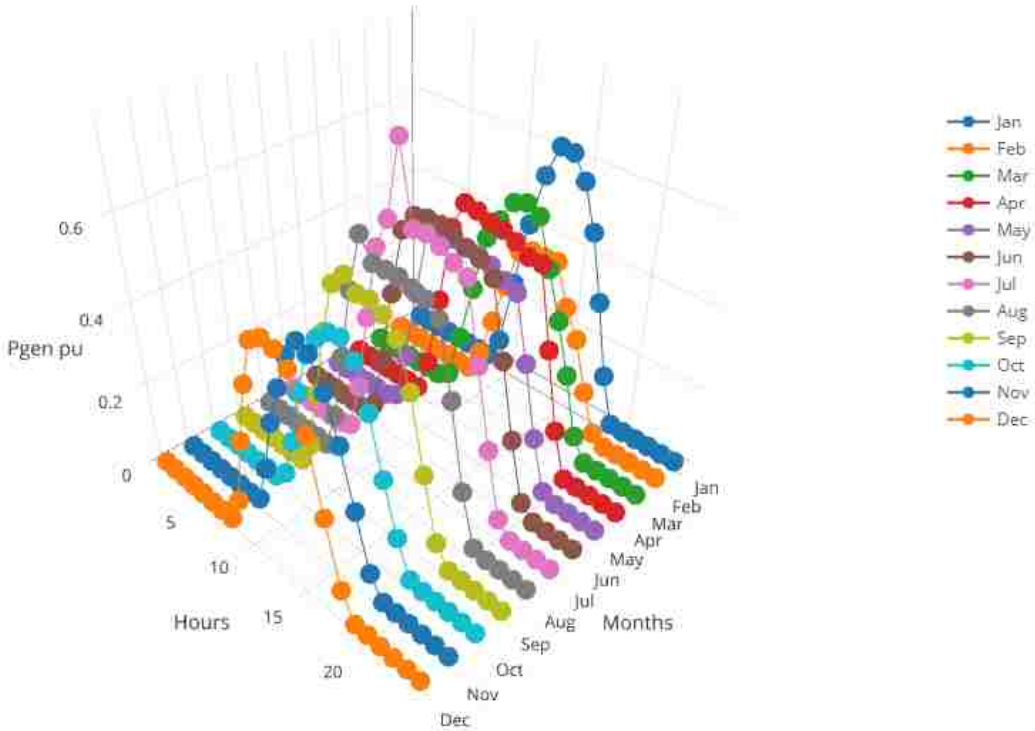

Figure 7.3: PV production for Case1 (PV only at Bus 6 (loc7))

higher at Bus 6 (loc7) after the installation of PV which is reasonable.

7.2.2 Case 2: PV and electric storage at Bus 6 (loc7)

In this case DER-CAM was allowed to pick up an optimized solution for both PV installation and electric storage at Bus 6 (loc7). DER-CAM picked up 8.84 MV of PV installations on the site of area 57815.6 m^2 area, however did not pick up electric storage. As the result, similar results as in Case 1 were obtained from this case too. Total of 15020.46 MWh of electricity was generated from the installation of PV. The optimized total costs of energy was reduced to €9.25M, with €1.13M of that being from PV installations. With the above specified capacity of PV running,

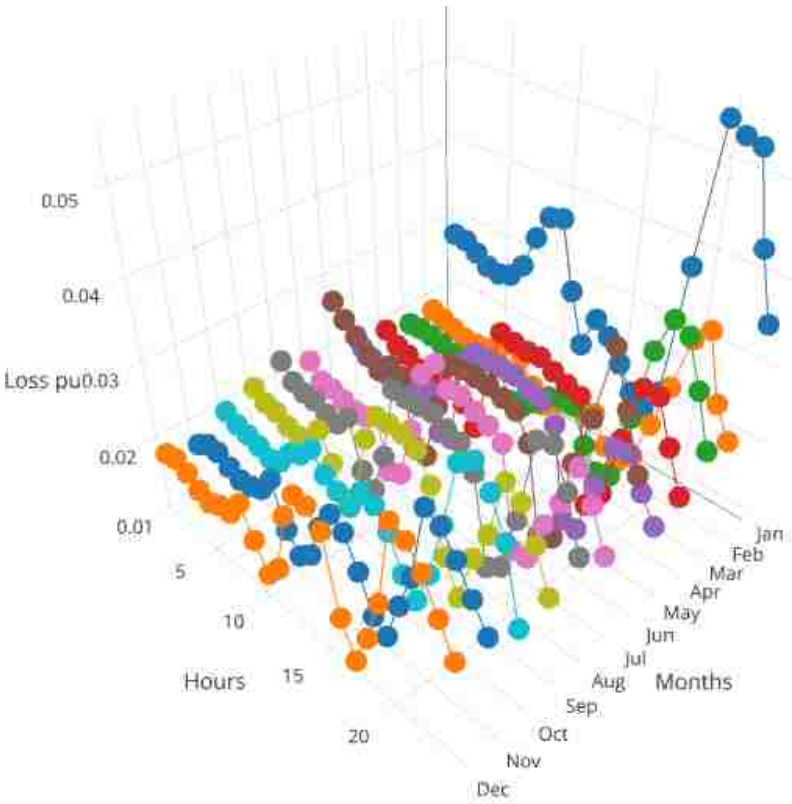

Figure 7.4: Power loss in pu for Case1 (PV only at Bus 6 (loc7))

electricity generated by the diesel generators decreased to 41112 MWh and the fuel (diesel) consumption reduced to 108789 MWh per year. CO_2 emissions was also subsequently reduced to 2.71×10^7 kg just like in Case 1. The slight difference were because of error tolerance in DER-CAM.

7.2.3 Case 3: PV only at Bus 7 (loc8)

In this third case, DER-CAM was allowed to pick up an optimized solution for only PV installation at Bus 7 (loc 8), just like before. The place was at the farthest end of Feeder 1 on the west side of the island and close to Bus 6. And also, since the

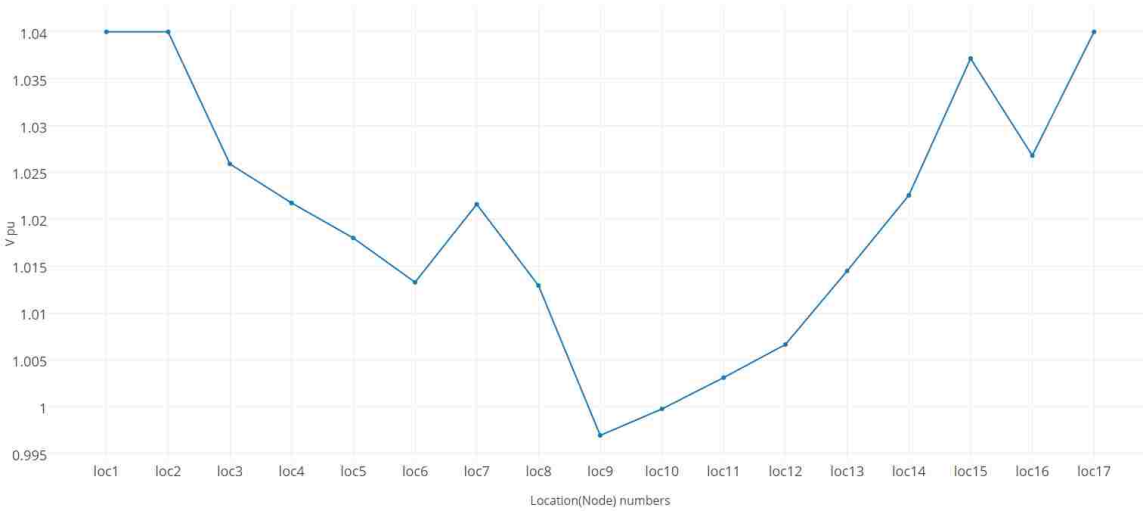

Figure 7.5: Real Voltage(pu) for Case1 (PV only at Bus 6 (loc7))

place was fairly close to the sea transportation of technologies was assumed to be convenient as well.

DER-CAM picked up 11.09 MW of PV installations on the site of area 72554.5 m^2 area. Total of 18008.3 MWh of electricity was generated from the installation of PV. Total costs of energy was reduced to €9.08M, with €1.41M of that being from PV installations. Figure 7.6 showed the hourly PV production for each months. With the specified capacity of PV running, electricity generated by the diesel generators decreased to 38175 MWh and the fuel (diesel) consumption reduced to 101179 MWh per year. Emissions was also reduced to 2.52×10^7 $kgCO_2$.

Figure 7.7 shows the plot of total losses in the network during peak load condition. From the graph, maximum loss was found to be 0.0545 pu (545kW) during peak load at Jan 20th hour. The installation of PV at Bus 7 have reduced the maximum distribution loss of the network. Figure 7.8 shows the voltage profile across all the locations (nodes). It was observed that voltage went higher at Bus 7 (loc8) after the installation of PV which is reasonable.

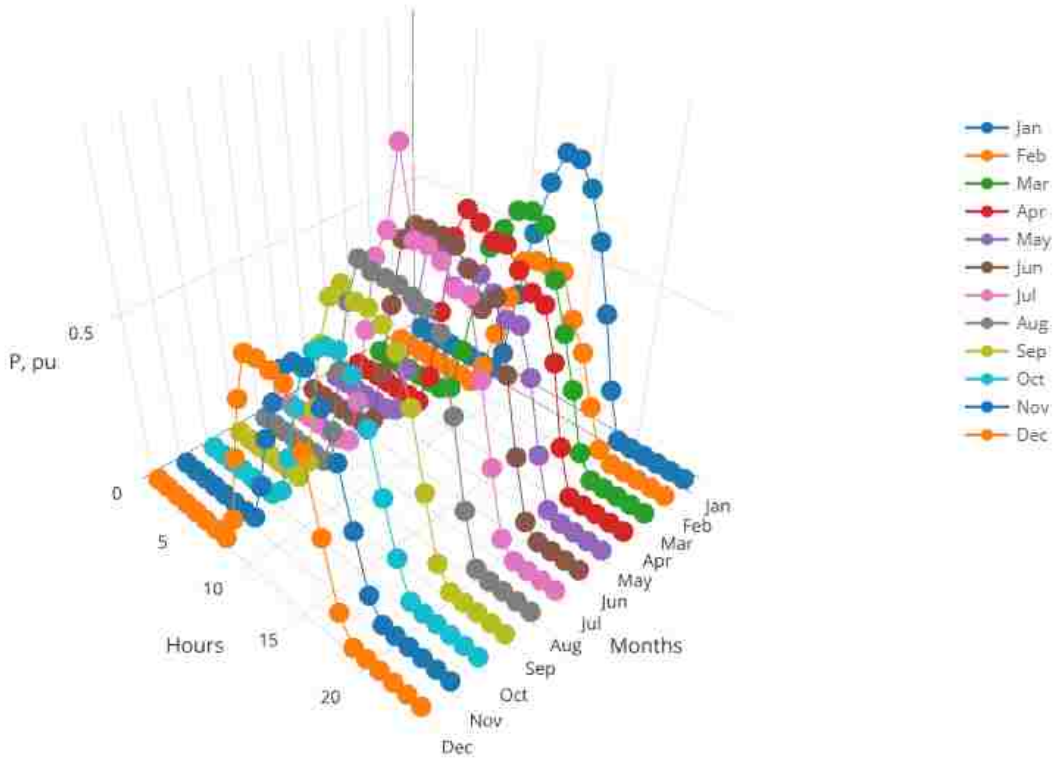

Figure 7.6: PV production for Case3 (PV only at Bus 7 (loc8))

7.2.4 Case 4: PV and electric storage at Bus 7 (loc8)

Case 4 was similar to what was done in earlier Case 3 one except DER-CAM was allowed to pick up electric storage together with PV for Bus 7. After the run, DER-CAM picked up 10.89 MW of PV installations on the site of area 71242 m^2 area and no battery. Because of no battery selection, the results were expected to be same as in Case 3 but was slightly (negligibly). Total of 17925.76 MWh of electricity was generated from the installation of PV. The total costs of energy was reduced to €9.07M, with €1.389M of that being from PV installations. Electricity generated by the diesel generators decreased to 38256.8 MWh and the diesel consumption reduced to 101412 MWh per year. CO_2 emissions was also subsequently reduced to 2.53×10^7

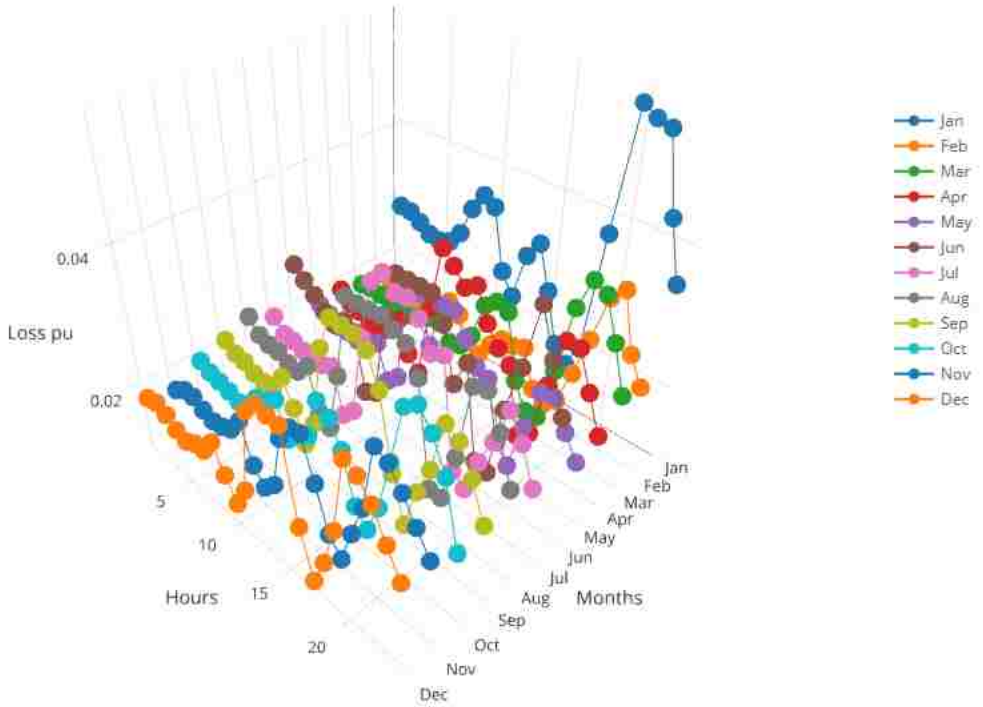

Figure 7.7: Power loss in pu for Case3 (PV only at Bus 7(loc8))

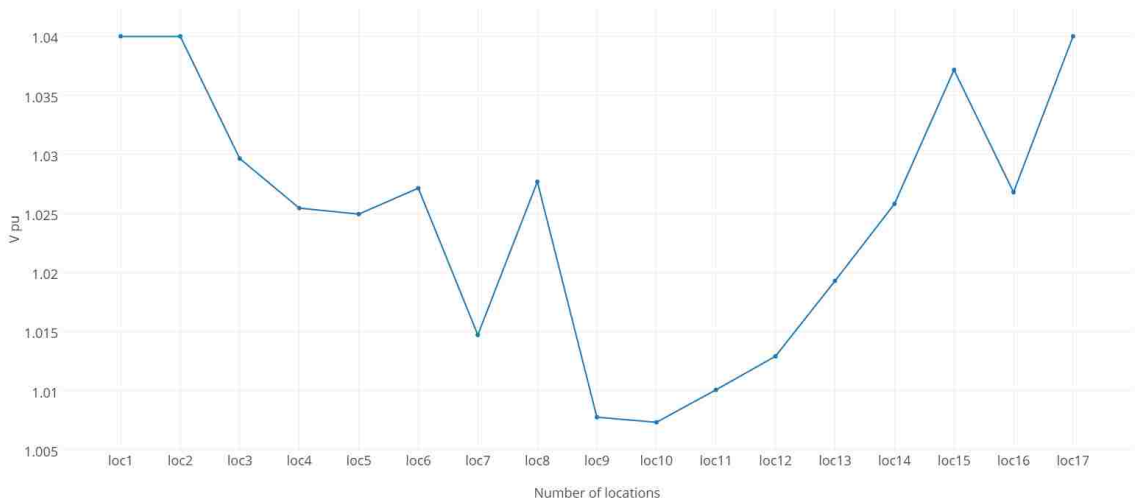

Figure 7.8: Real Voltage(pu) for Case3 (PV only at Bus 7 (loc8))

kg.

7.2.5 Case 5: PV only at Bus 3 (loc4)

After considering at the feasibility of PV and batteries at Bus 6 (loc7) and Bus 7 (loc8), a similar optimization run was done for Bus 3 (loc4). In this case DER-CAM was allowed to pick up an optimized solution for PV installation just like before. The place was at southern most part of Feeder 2.

DER-CAM picked up 5.94 MW of PV installations on the site of area 38828.32 m^2 area. Total of 10027.45 MWh of electricity was generated from the installation of PV. The new optimized total costs of energy was reduced to €9.68M, with €0.757M of that being from PV installations. Figure 7.9 shows the hourly PV production for each months. Electricity generated by the diesel generators decreased to 46149.5 MWh and the fuel consumption reduced to 121901 MWh per year. Emissions also reduced to $3.041X10^7$ $kgCO_2$.

The plot of total losses in the network during peak load conditions is shown in Figure 7.10. From the graph, maximum loss was found to be 0.0625 pu (625kW) during peak load at Jan 11th hour. The maximum distribution loss of the network was reduced from 731 kW-that was during peak load at Jan 11th hour- by 186kW. Figure 7.11 shows the voltage profile across all the locations (nodes). The voltage actually went higher at loc4 after the installation of PV.

7.2.6 Case 6: PV and Batteries at Bus 3 (loc4)

This case was same as above Case 5 plus DER-CAM was allowed to pick up an optimized solution for electric storage too. DER-CAM picked up 6.03 MW of PV installations on the site of area 39467.2 m^2 area and no battery. Total of 10388.9

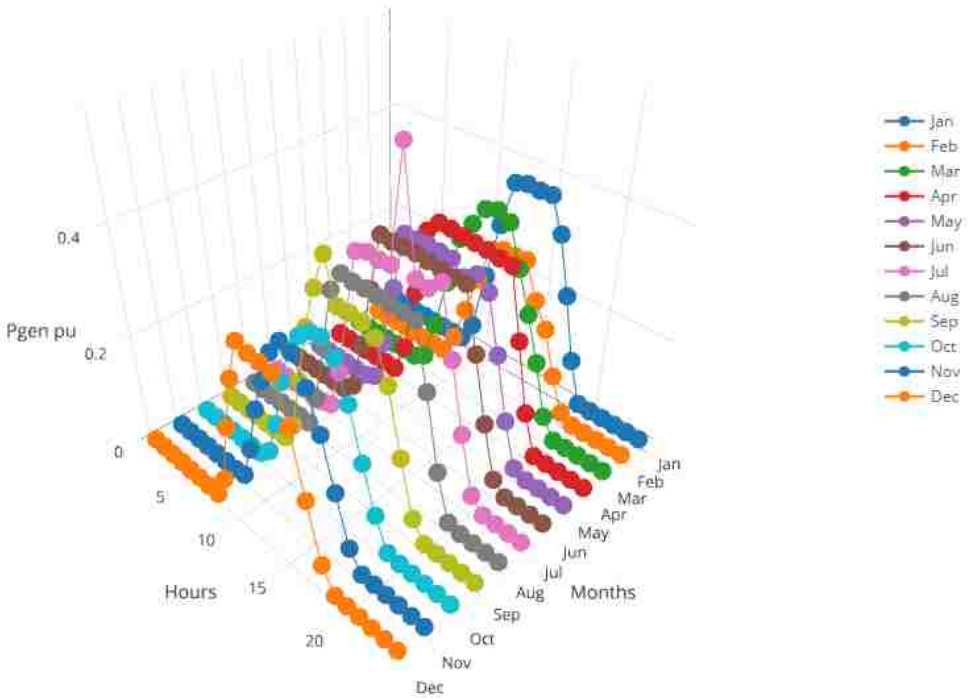

Figure 7.9: PV Generation for Case5 (PV only at Bus 3(loc4))

MWh of electricity was generated from the installation of PV. The new optimized total costs of energy was now reduced to €9.749M, with €0.8556M of that being from PV installations. Electricity generated by the diesel generators decreased to 45948.06 MWh and the fuel consumption reduced to 121410.75 MWh per year. CO_2 emissions was also subsequently reduced to 3.0289×10^7 kg. The results were almost same as in the Case 5 with the slight difference.

7.2.7 Case 7: PV only at Bus 10 (loc11)

The final location for looking at optimized installation of DERs was at Bus 10 (loc11). It was situated at the northern part of island in the mid-part of Feeder 1 and close to sea. This Case 7 was run to allow DER-CAM to pick up an optimized solution

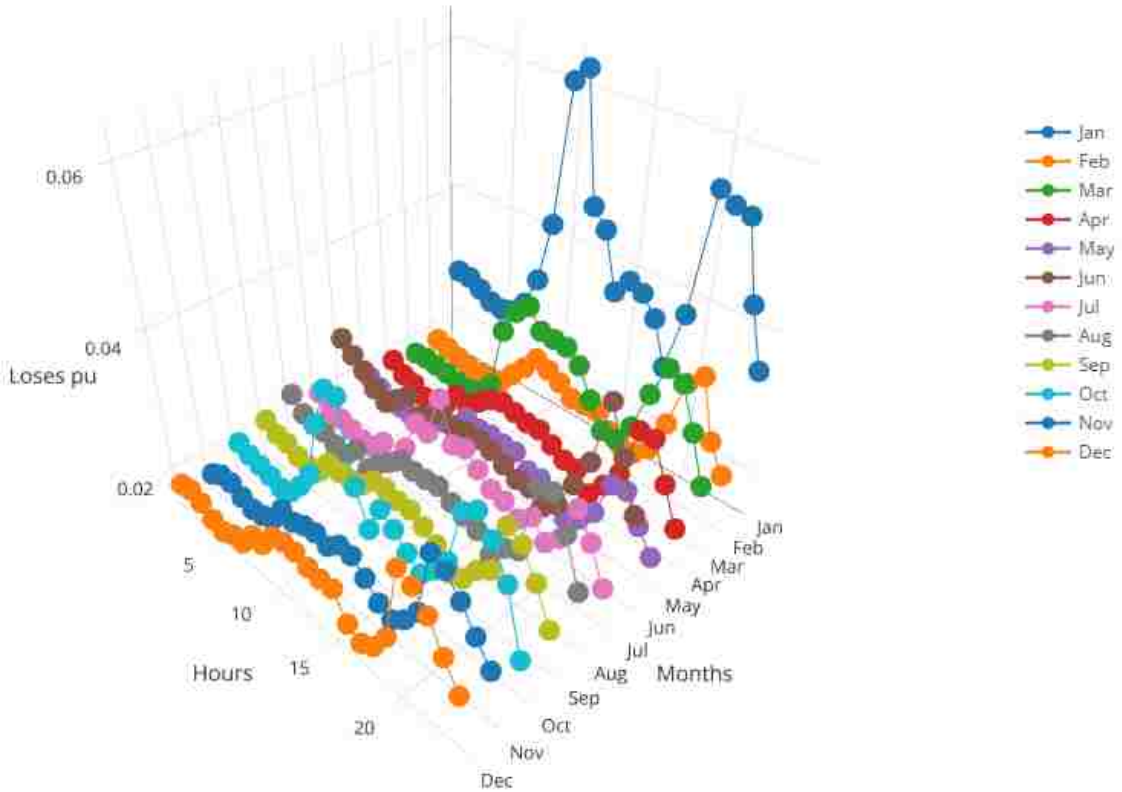

Figure 7.10: Distribution Loss (pu) for Case5 (PV only at Bus 3(loc4))

for PV only.

DER-CAM picked up 10.8 MV of PV installations on the site of area 70658.32 m^2 area. Total of 18168.45 MWh of electricity was generated from the installation of PV. The total costs of energy was now reduced to €9.064M, with €1.378M of that being from PV installations. Figure 7.12 shows the hourly PV production for each months.Total electricity generated by the diesel generators decreased to 48264.8 MWh and the diesel consumption reduced to 101479 MWh per year. It also caused the emissions to be reduced to 2.5317×10^7 kg CO_2.

Figure 7.13 shows the plot of total losses of the network during peak load conditions. From the graph, it was seen that the maximum loss was 0.0638 pu (638kW)

Figure 7.11: Voltage (pu) for Case5 (PV only at Bus 3(loc4))

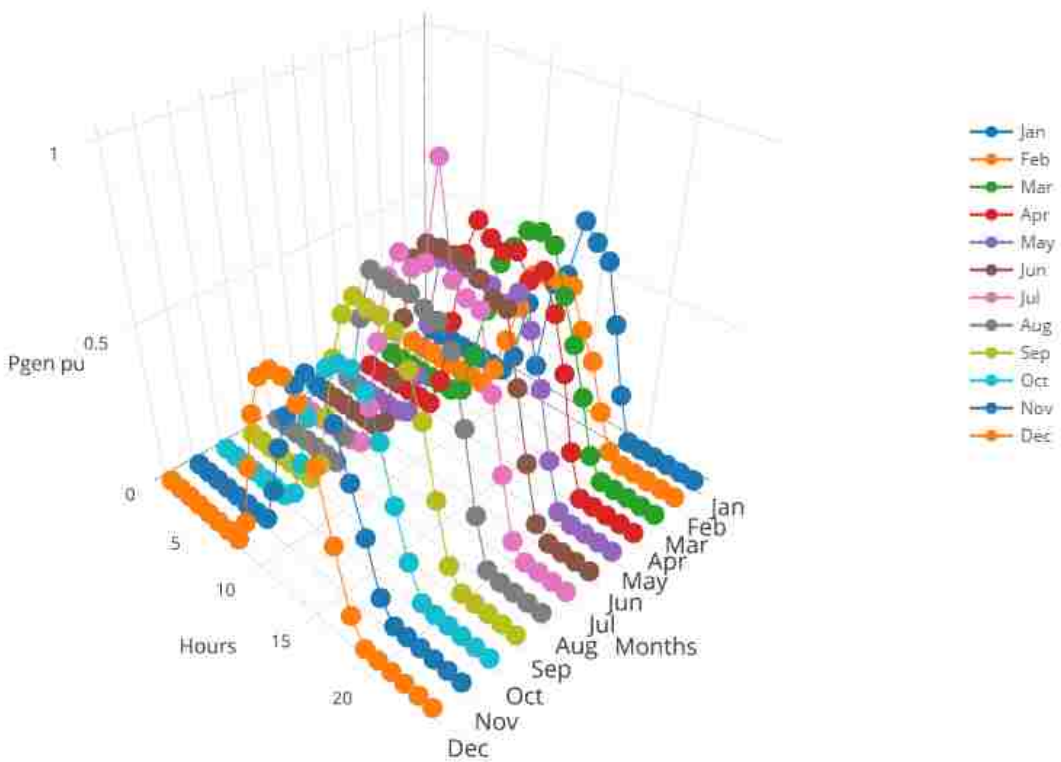

Figure 7.12: PV Generation for Case7 (PV only at Bus 10 (loc11))

during peak load at Jan 11th hour. The maximum distribution loss of the network was reduced from 731 kW-that was during peak load at Jan 11th hour- by 93kW. Voltage profile across all the locations (nodes) during Jan 11 AM peak-load condi-

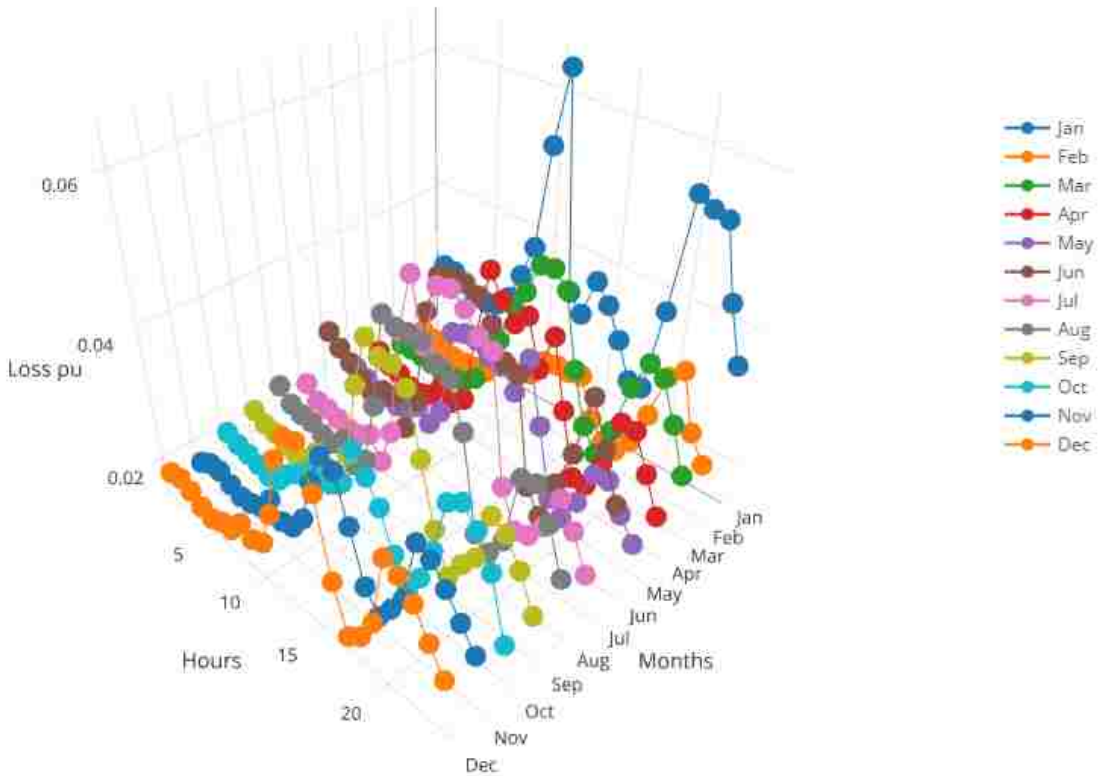

Figure 7.13: Distribution Loss (pu) for Case7 (PV only at Bus 10 (loc11))

tion was found as shown in Figure 7.14. It was observed that voltage actually went higher at loc4 after the installation of PV which is reasonable.

7.2.8 Case 8: PV and electric storage at Bus 10 (loc11)

Another similar optimization run was done for Bus 10 (loc11) where DER-CAM was allowed to pick up an optimized solution for both PV and electric storage installation. DER-CAM picked up 10.8 MV of MW installations on the site of area 70811.7 m^2

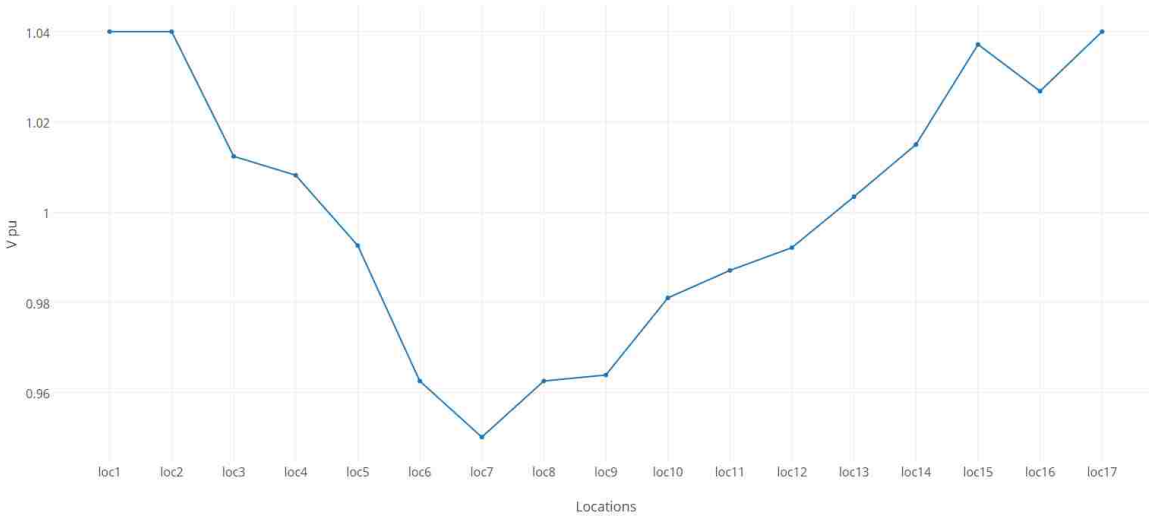

Figure 7.14: Voltage (pu) for Case7 (PV only at Bus 10 (loc11))

area and no battery. The results were observed almost similar with slight changes. Total of 18158.45 MWh of electricity was generated from the installation of PV. Total costs of energy was reduced to €9.065M, with €1.38M of that being from PV installations. Electricity generated by the diesel generators decreased to 3.8276 MWh , fuel consumption reduced to 101466 MWh per year and emissions was also subsequently reduced to 2.53×10^7 $kgCO_2$.

7.2.9 Case 9: PV and batteries at loc4, loc7, loc8 and loc10

After running separate optimization cases in different locations, in this case DER-CAM was allowed to pick up both PV and batteries in all the above mentioned locations: Bus 3 (loc4), Bus 6 (loc7), Bus 7 (loc8) and Bus 11 (loc10).

DER-CAM picked up 2.99 MW of PV at Bus 3 (loc4), 3.45 MW at Bus 6 (loc7), 2.1 MW at Bus 7 (loc8) and 3.18 MW at Bus 10 (loc11). Altogether, total of 10027.45 MWh of electricity was generated from the total 11.72 MW installation of PV but no batteries got selected by DER-CAM. The table for the size of PV installed in those

locations along with the area used and electricity generated in kWh was shown in Table 7.2.

Table 7.2: PV installations and their operations for Case 9

	Size (MW)	Area ($m\hat{2}$)	Gen kWh
loc4	2.99	19616.18	4055.85
loc7	3.45	22601.77	6773.61
loc8	2.1	13747.46	4120.03
loc11	3.18	20856.42	6250.54

With the above specified capacity of PV running, electricity generated by the diesel generators decreased to 36320.5 MWh and the fuel consumption reduced to 96167 MWh per year. Emissions also got reduced to 2.399×10^7 kgCO_2. The total costs of energy for a year was altogether €8.86M.

Figure 7.15 showed the plot of total losses in network during peak load conditions. From the graph, maximum loss was found to be 0.16438 pu (1.6438 MW) April 11 AM peak loads. However, the distribution losses at the time when it was maximum during Base Case run that at Jan 11 AM peak was merely 0.0241 pu (241 kW). In this case, total power generated by PV at April 11 AM was 7.84 MW whereas the peak load demand was 7.35 MW, so the PV production was higher than the load itself.

Figure 7.16 showed the voltage profile across all the locations (nodes). The overall voltage profile went higher with the installation of PV and various locations.

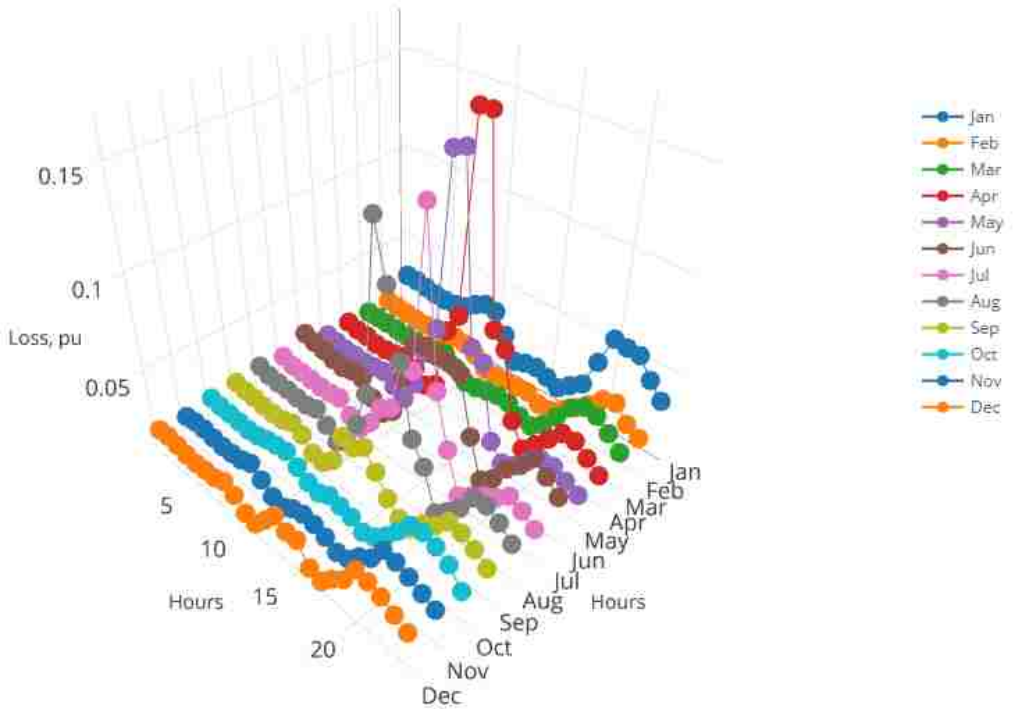

Figure 7.15: Distribution Loss (pu) for Case9 (PV and ES at loc4, loc7, loc8 and loc11)

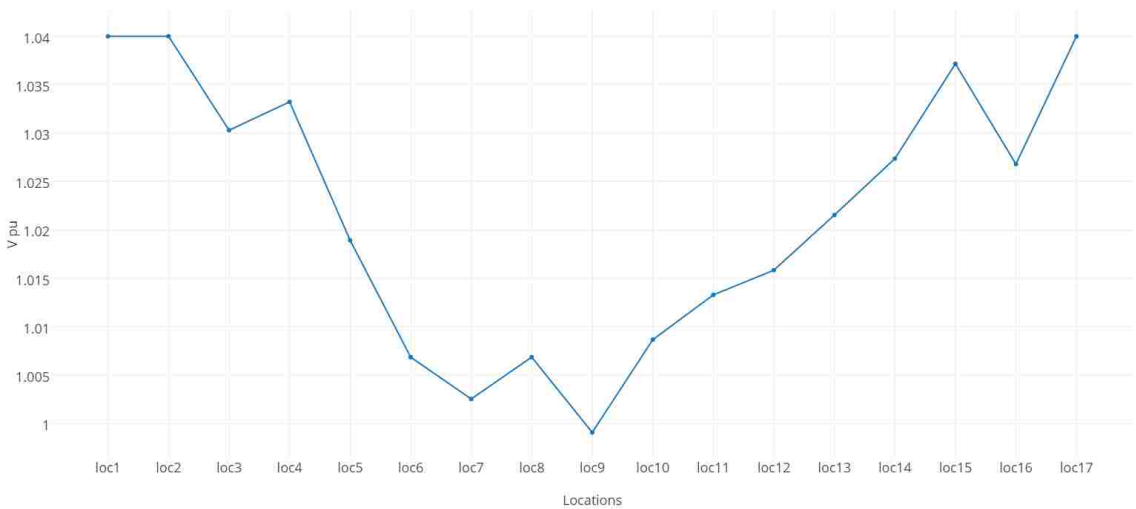

Figure 7.16: Voltage (pu) for Case9 (PV and ES at loc4, loc7, loc8 and loc11)

7.3 Analysis of Results

7.3.1 Summary of Investments and Installations

The different cases run in DER-CAM gave out different schemes of DERs installations at specified locations. As the DER-CAM deployed higher capacity of them, the total energy costs per annum was found to be decreasing which was the purpose of the optimization. Table 8.3 as shown below is the summary of total energy costs for each cases and their deployment of DERs.

Table 7.3: Summary of Investments and Installations

Case	PV (MW)	ES (MWh)	Total Energy Costs (€M)
0	0	0	10.55
1	8.85	0	9.25
2	8.84	0	9.25
3	11.09	0	9.08
4	10.89	0	9.07
5	5.94	0	9.68
6	6.03	0	9.75
7	10.08	0	9.06
8	10.08	0	9.06
9	11.72	0	8.86

As shown in the table, the Base Case where there were no DERs deployment total energy costs was €10.55M which was the highest of all. Later on when DER-CAM was allowed to pick up the optimized installations of DERs, the cost decreased which showed that it would be cost optimized to install resulted sizes of them. Among the cases, Case 9 where DER-CAM was allowed and picked up subsequently the DERs in all four locations (Loc4, Loc7, Loc8 and Loc11) was the most cost effective due to its least total energy costs of merely €8.86M. As discussed in each cases, these reductions in total costs of energy were direct result of decrement in consumption of fuel as the result of electric energy generation from installed DERs. In this way,

the results of what size of installations at which locations would optimize the total energy costs per year were obtained from DER-CAM.

However, one significant point noted while running these cases was that DER-CAM did not pick any size of electric storage (ES) in any of the cases. The capital cost of battery was high for economic deployment.

7.3.2 Summary of Voltage profiles and Distribution Losses

The primary objective of this optimization project was to reduce the total costs of energy with the installations of DERs. To carry out this, DER-CAM was expected to work on reducing the distribution losses as well. Another advantageous aspect of DER-CAM optimization was improving voltage profile too as the buses where DERs were installed were expected to have higher voltage than before, and we selected the installation locations close to big load centers which generally have voltage dip. Following table show the distribution losses and minimum and maximum voltages in pu for different cases.

Table 7.4: Minimum and maximum voltage(pu) for different optimization cases

Case no.	Vmin pu	Vmax pu
0	0.944 (loc7)	1.04 (loc1)
1	0.997 (loc7)	1.04 (loc1)
2	0.997 (loc7)	1.04 (loc1)
3	1.007 (loc10)	1.04 (loc1)
4	1.007 (loc10)	1.04 (loc1)
5	0.955 (loc7)	1.04 (loc1)
6	0.955 (loc7)	1.04 (loc1)
7	0.949 (loc7)	1.04 (loc1)
8	0.949 (loc7)	1.04 (loc1)
9	0.999 (loc7)	1.04 (loc1)

Table 7.4 showed the maximum and minimum voltage values in per unit across the whole network. The minimum value of voltage all over the network was 0.944 pu

Table 7.5: Distribution Losses for different optimization cases

Case no.	Peak Losses (kW)	Losses at Peak Load (kW)
0	735 (Jan 11 AM Peak)	735 (Jan 11 AM Peak)
1	545 (Jan 8 PM Peak)	279 (Jan 11 PM Peak)
2	545 (Jan 8 PM Peak)	279 (Jan 11 PM Peak)
3	545 (Jan 8 PM Peak)	254 (Jan 11 PM Peak)
4	545 (Jan 8 PM Peak)	254 (Jan 11 PM Peak)
5	625 (Jan 11 AM Peak)	625 (Jan 11 AM Peak)
6	625 (Jan 11 AM Peak)	625 (Jan 11 AM Peak)
7	638 (Jan 11 AM Peak)	638 (Jan 11 AM Peak)
8	625 (Jan 11 AM Peak)	625 (Jan 11 AM Peak)
9	1643.8 (Apr 11 AM Peak)	241 (Jan 11 AM Peak)

which was at loc7 (Bus 6) during the Base case. It was later found to be increased to different extents depending upon the optimized integration of PV in various locations. The voltage at the location increased when the installation was done right at the Bus 6 (loc7) and Bus 10.

Table 7.5 showed the distribution losses at different optimization cases. The biggest loss was 735 kW at peak load of January 11 AM in Base Case run. The loss was then decreased to different extents with the optimized integration of PV in various locations. The minimum peak loss was found to be 545 kW (except in Case 9) when PV was introduced in Bus 6 and Bus 7 as in Case 1 to Case 4. It was assumed that the integration of DERs near the load centers reduced the distribution losses and that was a part of a reason for DER-CAM picking up the right size of installation. However, in the Case 9 where DER-CAM was allowed to pick up the installation of PV and ES at all those four locations, the peak loss was found to be at 11 AM of April where it was 1.64 MW, and that was way more than that in Base Case run despite lower total costs of energy.

On the other side, distribution losses at peak load condition of the network (January 11 AM peak) were all lower than that in Base Case run. The loss decreased up to 241 kW when PV was installed at all four locations despite the peak loss at that

case being as big as 1.64 MW.

7.3.3 Summary of Fuel Consumption and CO_2 Emissions

During the various cases of optimization of PV and ES integration into the grid, amount of diesel fuel consumption by the generators was found to be varying as the DERs shared the generation burden. That subsequently resulted on the decrease in CO_2 emissions as well.

Table 7.6: Summary of Fuel Consumptions and CO_2 Emissions

Case	Diesel Consumption (MWh)	Fuel Costs (€M)	CO_2 emissions ($\times 10^7$ kg)
0	148775	8.17	3.71
1	108769	5.97	2.71
2	108790	5.97	2.71
3	101179	5.55	2.54
4	101412	5.55	2.53
5	121901	6.69	3.04
6	121410	6.67	3.03
7	101479	5.57	2.53
8	101466	5.57	2.53
9	96167	5.28	2.39

Table 7.6 gave the information about the diesel fuel consumption by the generators in equivalent MWh in each cases. It can be noted that 148.7k MWh equivalent of Diesel was consumed to supply the loads in Base Case. Consumption was then decreased after the subsequent integration of PV in the following cases. The least consumption was noted for Case 9 which had the highest size of PV installed and as expected had the lease cost of fuels too. CO_2 emissions was also highest for the Base Case (Case 0), about 3.71 x10^7 kg. The emissions subsided along with the integration of PV and decrement of diesel fuel consumption. With the scheme of Case 9, the emission of CO_2 was reduced up to 2.39x10^7 kg.

7.4 Different cases of battery installation

DER-CAM did not pick up any batteries in any of the above cases with its capital cost at €500/kWh: the cost of battery was too high for economic deployment. Also, the tax on CO_2 were neglected for above cases which did not help battery deployment either.

With the increase on CO_2 tax, the generators will be on decreased priority to be picked up by DER-CAM. Consequently, the need for supply-load leveling will be of greater importance. The integration of PV would be highly prioritized which was expected to favor the deployment of battery. Varying costs of battery were analyzed to see at what conditions their deployment would be financially feasible. The tax on CO_2 emissions was set at €100/kgCO_2 and DER-CAM was run with Base Case that is without any DERs installation. The total costs of energy was €14.14M.

With capital cost of battery reduced as low as €150/kWh, DER-CAM was allowed to pick up both PV and battery at Bus 6 as in Case 2 earlier. Doing this, 13.7 MW of PV was installed together with battery of 22.7 MWh. The installations reduced the total costs of energy down to €11.77M.

When the same case was run with capital cost of battery increased to €175/kWh, DER-CAM picked up 10.3 MW of PV and 5.8 MWh of battery with total cost of energy €11.94M.

Finally, a case allowing DER-CAM to pick up PV and batteries at loc4, loc7, loc8 and loc11(like in Case 9 above) with capital cost of battery set to zero and no CO_2 emission tax was run in DER-CAM. The purpose of this case was to see how would battery help the deployment of PV and increase the penetration level of them in microgrid if it were for free. Doing so, the total cost of energy came down to €3.44M. The total of 26.71 MW of PV and 140.76 MWh of batteries were installed in

those four locations. The size of battery picked up by DER-CAM was certainly very high because of its zero cost. Table 7.7 shows the installment of PV and batteries in various locations. With the high battery installations, the size of installed PV was also found to be bigger.

Table 7.7: PV and battery at loc4, loc7, loc8 and loc11 with no battery capital cost

	PV (MW)	ES (MWh)
loc4	7.86	49.5
loc7	0	8.06
lco8	14.7	83.2
lco11	4.15	0
Total	26.71	140.76

Chapter 8

Conclusions

This thesis was focused on finding optimized placing and sizing of DERs (PV and battery) on a microgrid of La Gomera island so that the total cost of energy and emission would be less than what currently is. To find the optimized solutions, DER-CAM was used to model the microgrid and run different cases of integration of PV and battery at various locations.

In Chapter 2, the current energy scenario of La Gomera, existing microgrid, electric distribution network and specific purpose of the thesis were discussed. La Gomera was mostly dependent on fossil fuel for energy and very small part (about 1%) of electric energy came from renewable resources. Different tools and techniques to model a microgrid and optimize it including the operation of DER-CAM and the power flow approximation techniques used by it were described.

In chapter 3, information provided from EPRI and utility company operating on the island were studied. The electrical network properties and power flow results were by EPRI from the modeling and simulation of the microgrid in PSSE. Generation characteristics, load at feeder lines and electric network properties that were required to model the microgrid in DER-CAM were discussed. The results from PSSE were

set as reference for benchmarking the results from DER-CAM to ensure that the modeling and power flow results in DER-CAM were reasonable.

In Chapter 4, the information as discussed in Chapter 3 was used to characterize and model the microgrid. One line diagram was formulated from the nodal information provided from the simulation in PSSE and the network properties in terms of lengths, branch capacities, admittance and impedance matrices were computed. Load data at given feeder lines were modeled into different load centers and processed into the format as required by DER-CAM. Characteristics of generators were determined from the data of their operations as provided by the utility company.

In chapter 5, the modeled microgrid was run in DER-CAM to compare power flow results with those from PSSE. For this purpose, nodal voltages and distribution losses were compared. The difference on the nodal voltages given by PSSE and DER-CAM was not more than 6.7% and hence the modeling of microgrid was found reasonable. Also the calculated distribution loss of 5.7% was lower than the reported 8.7% but was considered reasonable because of omission of reactive load in DER-CAM. Then in chapter 6, the system was reconfigured with the addition of previously omitted feeder lines to make the modeling of microgrid close to the existing system.

In chapter 7, financial and electrical specifications of PV and battery along with weather data like solar insolation and ambient temperature that effects the performance of PV were discussed. After identifying four suitable locations, different cases of PV and battery installations at those locations were run in DER-CAM. Results of these optimization cases such as size of installation, total costs of energy, emissions and power flow results were studied for all the cases. The cases were compared with each other in terms of the size of installation of PV and batteries, total costs of energy, distribution losses and emissions. DER-CAM picked up optimized size of PV installation at specified locations but batteries were not picked up at all in any of locations. The case where DER-CAM was allowed to install PV and battery at

all four locations was found to me the optimal solution in terms of total costs and emissions. Some cases with lower costs of battery and high tax on emissions were run to see DER-CAM pick up batteries.

Installation of PV at those four locations close to big load centers was found to be most cost effective and had least CO_2 emissions. Total cost of energy per year was reduced by 16% and emission by 36%. The distribution loss at peak load was reduced by about 67%. The capital cost of the battery was found be too high for economic deployment as DER-CAM did not pick up any batteries in any of the cases. In this way, the optimized sizes and places for installation of PV and batteries were computed using DER-CAM. The installation was found to reduce the total costs of energy and emissions as wished by the utility.

DER-CAM was an efficient tool to model a microgrid and optimize the integration of DERs in microgrid. The approximated results from DER-CAM were reasonably comparable with the simulated results from PSSE. However, working on it had a lot of challenges and implications. The results were very sensitive to the quality of inputs and it took long time to run with higher accuracy. De-bugging and output results visualizing were very tedious and time-consuming due it its interface.

Future work

In order to model the microgrid system even more closely, the reactive load should be taken into account while modeling the load. We omitted the reactive load because of limitations in DER-CAM at the time of work. DER-CAM should be modified to include the reactive loads that would give even more accurate results for power flow studies and optimization.

Based on the results of DER-CAM, the sites for the installation of PV have to be

evaluated before actual deployment of PV. We only evaluated those locations based on their location and accessibility which might not be enough for real installation.

With DER-CAM suggesting installation of large PV farms, it would be desired to perform dynamic system simulation to asses the voltage fluctuation in microgrid because of high PV integration. Necessary control mechanisms have to be determined to mitigate the possible effect of high PV penetration.

Bibliography

[1] URL: http://energy.sandia.gov/energy/ssrei/gridmod/renewable-energy-integration/smart-grid-tools-and-technology/.

[2] URL: http://www.homerenergy.com/software.html.

[3] URL: http://photovoltaics.sandia.gov/docs/Database.htm.

[4] *ACTION PLAN FOR SUSTAINABLE ENERGY ISLAND LA GOMERA ISLAND (2012-2020)*. URL: http://www.islepact.eu/userfiles/ISEAPs/Report/canary/ISEAP_La_Gomera.pdf.

[5] *Applying DER-CAM for IIT Microgrid Expansion Planning*. URL: https://building-microgrid.lbl.gov/sites/all/files/DER-CAM_IITMicrogridPlanning.pdf.

[6] Ashoke Kumar Basu et al. "Microgrids: Energy management by strategic deployment of DERs—A comprehensive survey". In: *Renewable and Sustainable Energy Reviews* 15.9 (2011), pp. 4348 –4356. ISSN: 1364-0321. DOI: http://dx.doi.org/10.1016/j.rser.2011.07.116. URL: http://www.sciencedirect.com/science/article/pii/S1364032111003637.

[7] S. Bolognani and S. Zampieri. "On the Existence and Linear Approximation of the Power Flow Solution in Power Distribution Networks". In: *IEEE Transactions on Power Systems* 31.1 (2016), pp. 163–172. ISSN: 0885-8950. DOI: 10.1109/TPWRS.2015.2395452.

[8] *Central térmica El Palmar*. URL: https://es.wikipedia.org/wiki/Central_t%C3%A9rmica_El_Palmar.

[9] *Costs of Utility Distributed Generators, 1-10 MW: Twenty-Four Case Studies*. Technical Results. EPRI.

[10] *DER-CAM Overview*. URL: https://building-microgrid.lbl.gov/sites/all/files/projects/DER-CAM%20Presentation%2012%20May%202016.pdf.

[11] *DIRECTIVE 2009/28/EC OF THE EUROPEAN PARLIAMENT AND OF THE COUNCIL*. URL: http://eur-lex.europa.eu/legal-content/EN/ALL/?uri=CELEX%3A32009L0028.

[12] *Distributed generation*. URL: https://en.wikipedia.org/wiki/Distributed_generation.

[13] Ulas Eminoglu and M. Hakan Hocaoglu. "A new power flow method for radial distribution systems including voltage dependent load models". In: *Electric Power Systems Research* 76.1–3 (2005), pp. 106 –114. ISSN: 0378-7796. DOI: http://dx.doi.org/10.1016/j.epsr.2005.05.008. URL: http://www.sciencedirect.com/science/article/pii/S0378779605001677.

[14] *European 20-20-20 Targets*. URL: http://www.recs.org/glossary/european-20-20-20-targets.

[15] John F Franco et al. "A mixed-integer LP model for the reconfiguration of radial electric distribution systems considering distributed generation". In: *Electric Power Systems Research* 97 (2013), pp. 51–60.

[16] *La Gomera*. URL: https://en.wikipedia.org/wiki/La_Gomera.

[17] Rodrigo H. de Luis. "Optimal Placement and Sizing of Distributed Generation". Master's Thesis. TUDelft.

[18] M.S. Mahmoud, S. Azher Hussain, and M.A. Abido. "Modeling and control of microgrid: An overview". In: *Journal of the Franklin Institute* 351.5 (2014), pp. 2822 –2859. ISSN: 0016-0032. DOI: http://dx.doi.org/10.1016/j.jfranklin.2014.01.016. URL: http://www.sciencedirect.com/science/article/pii/S0016003214000180.

[19] *Microgrids – Benefits, Models, Barriers and Suggested Policy Initiatives for the Commonwealth of Massachusetts*. DNV KEMA. URL: http://nyssmartgrid.com/wp-content/uploads/Microgrids-Benefits-Models-Barriers-and-Suggested-Policy-Initiatives-for-the-Commonwealth-of-Massachusetts.pdf.

[20] Michael Stadler et al. "Optimizing Distributed Energy Resources and Building Retrofits with the Strategic DER- CAModel". In: *Applied Energy* 132 (2014), pp. 556–567. ISSN: 0306-2619. DOI: 10.1016/j.apenergy.2014.07.041.